JOURNAL
OF
ENVIRONMENTAL GEOGRAPHY

2008
Vol. I. No. 1-2

ISSN 2060-3274

Editors wish to express their appreciation towards the anonymous reviewers of the articles included in the present issue.

Language quality of individual articles is the responsibility of authors.

CONTENTS

Journal of Env. Geogr. Vol. I. No. 1-2. pp. 5-10

EXTRACTION OF DIGITAL SURFACE MODELS FROM CORONA SATELLITE STEREO IMAGES

Mészáros, M.[1] – Szatmári, J.[2] – Tobak, Z.[2] – Mucsi, L.[2]

[1] University of Novi Sad, Faculty of Science, Departement of Geography Trg Dositeja Obradovica, Novi Sad, Serbia
[2]University of Szeged, Department of Physical Geography and Geoinformatics, 6722 Egyetem u. 2, Szeged, Hungary

Abstract

Satellite images can be utilised for observing surficial changes, especially efficient in the monitoring of larger areas. The comparative analysis of high resolution images from earlier periods with recent data can provide insight in the scale of changes in topography, and with meteorological, hydrological and other historic records, can lead to better understanding and more reliable modelling of the predominant processes causing mass movement.
More accurate morphometric and visual analysis of the topographic changes is possible using digital surface model (DSM), which can be obtained from satellite stereo images. In this paper, the authors evaluated methods of creation digital surface models obtained from satellite images from the CORONA program in monitoring surficial mass movement processes in the Fruška Gora mountain area, in the southern part of the Vojvodina province in Serbia. This area is of particular interest because of its favourable geographic location, rich geo- and cultural heritage and increasing demand for exploitation, which results in greater impact of natural hazards.
The CORONA images were chosen because of good availability of high resolution coverage for the whole area from the period of past four decades.

Keywords: remote sensing, Fruška gora, CORONA satellite images, automated digital surface model extraction

INTRODUCTION

By 2002 the Department of Geography, University of Novi Sad managed to establish bilateral relations with the Department of Physical Geography and Geoinformatics at the University of Szeged, Hungary, which opened up the possibility of mutual geomorphological studies via the application of geoinformatical tools. One major aim of this research project was the creation of a digital elevation model of the study area using reliable, yet the oldest available data sources. This model will be compared to a model recording the modern conditions of the area in order to evaluate any past changes. This new modern model is based on data recorded during field surveys and gained via the analysis of recent high-resolution satellite images.

For the accuracy of the investigations aerial photographs and satellite images used in the study must have a spatial resolution of at least 3 m. Such photos and images are lacking from Serbian official sources. However, we have come across a database of former CORONA spy satellites, where stereo image pairs could have been readily purchased of the study area. The present study gives an overview of the analysis of these images and the extraction of the DSM using the elucidated information.

STUDY AREA

The study area located along the river Danube north of the Fruška Gora is very similar in morphology to the loess areas of Paks and Dunaföldvár, in Central Hungary. These loess-covered Pleistocene surfaces located along the rivers are frequently subjected to landslides and mudslides. Although a detailed geographic survey of the mentioned study area was implemented as early as the end of the 19th century, these studies are no match to the complex geomorphological studies implemented on Hungarian loessy areas. Thus there are no historical records available for the observable landslides of the area. The only option for understanding the dynamics of these mass movement processes is to find information sources, enabling the preparation of digital elevation models for the past 40-50 years and compare them with those prepared on the basis of modern field data.

Satellite image analysis can yield limited results in the investigation of certain surficial processes, thanks to their periodic nature characterized by a relatively longer stasis. The only exception might be the relatively recent landslides, where high resolution images of the affected area prior and after the events are readily available. Areas along the Danube frequently subjected to landslides (e.g. the vicinity of Dunaföldvár) have enjoyed much attention by geomorphologists during the second half of the 20th century in Hungary, primarily related to the works of Pécsi (Pécsi M. 1991). These landforms are frequently observable in the Lower Danube area, especially in the vicinity of the city of Novi Sad and the northern foothills of the Fruška Gora (Tarcal or Köles Hills). Unfortunately, no matter how close this region was to the area of present day Hungary, the known political and other tensions; for example, war prevented Hungarian experts from joining the geomorphological investigations of the area.

Table 1 The main features of the cameras and film used during the KH-4B mission (Dashora A. et al. 2007)

System	*Corona KH-4B*
Time of recording	08.02.1969
Mission no.	1106
Orbit height	150 km
Camera type	Panoramic
Angle of twin cameras	30°
Focal length	609.6 mm
Film type	Panchromatic
Film resolution	160 line/mm
Actually usable film size	55.37 x 756.9 mm (mm x mm)
Area covered	14x188 km
Scale	1:247500
Field resolution	1.83 m

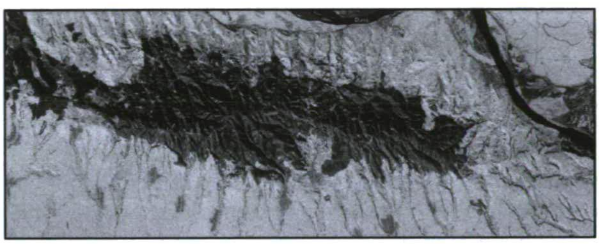

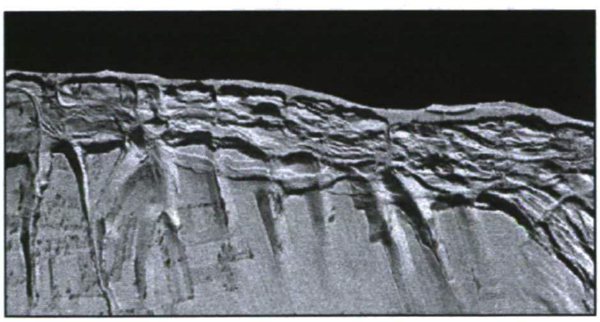

Fig. 1a-b The Fruška Gora hills and a landslide affected area on the right banks of the river Danube (SE of Novi Sad as seen on the CORONA image of 08.02.1969 (40x17 km)

APPLIED MATERIAL

In February 1995 US president Bill Clinton (1995) exempted from secrecy in a special resolution the satellite images taken by the spy satellites CORONA (KH 1-4), ARGON (KH-5), and LANYARD (KH-6). The resolution disclosed more than 860,000 images taken between 1960 and 1972. These images are open to the public and can be ordered from the USGS using the homesite of USGS EarthExplorer.

A stereo image analysis is somewhat hampered by the fact that parameters necessary for interior orientation is only partially known and exterior parameters are not available for the CORONA images. Thus it was necessary to review processing methods available for the CORONA images in the literature.

As part of the IMPETUS project (Altmaier A. – Kany C. 2002) DSM was prepared for an area of ca. 100 km^2 using stereo images of the CORONA KH-4B satellite over Morocco. To derive the ground control points a differential GPS technique was applied with an accuracy of 10 cm in *x*, *y* and *z* directions. Schenk T. et al. (2003) set up a camera model for the KH-4A/B systems using collinearity equations. The derived algorithm was tested using calibration points gained from a KH-4A stereo image pair and regular topographic maps of the study area. Field accuracy was tested via affine and polynomial transformation of the studied images.

Bayram B. et al. (2004) were tracing shoreline changes near Istambul using a CORONA image taken in 1963 and panchromatic SPOT-4 and IRS-1D images taken at the end of the 1990s. For the rectification of the KH-4A image pairs affine, projective and rubber sheet transformation methods were applied and evaluated in terms of field accuracy. All three studies arrived at the conclusion that CORONA images, in the form of stereo pairs are suitable for tracing surficial changes for the past 30-40 years, yielding sufficient accuracy and thrift, comparable to modern high resolution satellite images.

METHODS

Processing of satellite stereo images

Several time periods were found in the archive of the USGS (08.02.1969, 26.05.1972), when stereo images were taken for the mentioned study area (*Table 1*). From these the ones taken in 1969 had no cloud cover. The ordered negatives were scanned by colleagues of the Ministry of Defence Mapping Company at a resolution of 12 μm (*Figs. 1a-b*). In 2003 a single negative roll costed 18 USD.

For processing the ERDAS OrthoBase Pro digital photogrammetric software pack was utilized, and an approximative aerial triangulation result was found using such parameters as focal length, orbit height, film pixel size and ground control points. Perfectly accurate orientation requiring extreme computation power was practically unachievable (Schenk T. et al 2003). This was not our ultimate goal however, as we mainly aimed our work at deriving usable morphological data suitable for the preparation of digital surface models for geomorphological studies from these images, in an efficient and eco-

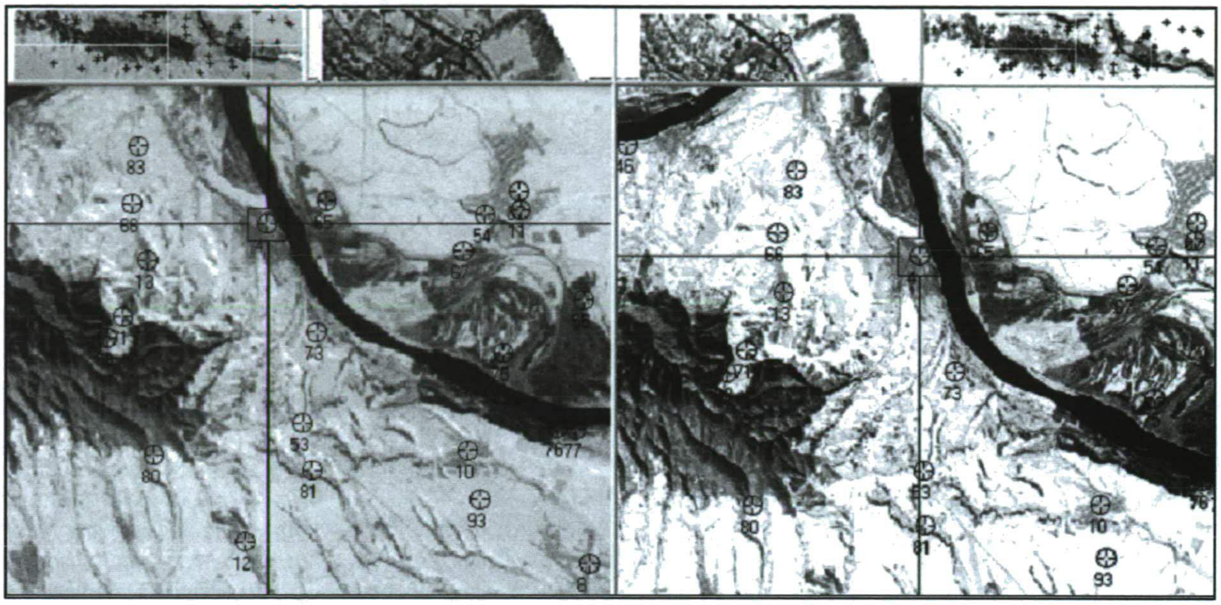

Fig. 2 The absolute orientation of the CORONA images using ground control points

nomic way to meet the expected accuracy requirements as well.

The next step was the relative orientation of the stereo image pair with using ca. 40 tie points. The automatic tie point generation method yielded no sufficient amount and quality of homologue points as the winter images were taken among conditions of partial suficial snow cover. The automatic matching algorithm thus could not identify homologue points on larger homogenous snow covered areas. In these areas tie points were measured manually.

For the exterior orientation, ground control points were recorded in the mountain and its foothills using relative rapid static GPS measurements (*Fig. 2*), the basis point was set up on the roof of the building hosting our department at Szeged.

The length of the baseline was ca. 145 km, ensuring a good accuracy for the image analysis. On the satellite images taken 36 years ago ca. 30 interest points were identified at crossings of paved roads, on the trajectory of creeks charging into the river Danube, and rails of bridges crossing the creeks and canals charging into the Danube. A good ground control point was found near the Iriski–Venac Monument located in the central, highest part of the Fruška Gora, which monument managed to survive the 1999 NATO bombings, unlike the TV tower, which stands as a stunning and saddening memento of futile clashes from the closure of the 20th century (*Fig. 3*).

The transformation of the GPS coordinates to the local reference system was not without any difficulties. An approximating solution was found to this problem (Timár G. et al. 2002, 2004). The development of a reliable coordinate transformation method for studying dynamic surface changes is a task to be solved in the future.

After the assignment of suitable control and tie points, an aerial triangulation was implemented using a

Fig. 3 The Novi Sad TV tower in 2004

self-calibrating direct linear transformation offered by the program (Altmaier A. – Kany C. 2002). This method does not require the knowledge of either the interior orientation data of the camera or the predicted exterior parameters. After multiple runs and the evaluation of the residuals for tie and control points as well as the RMS error values, the best outcome was chosen via elimination of points yielding the largest error from the numerous iterates.

Extraction of DSM

After this, a digital surface model (DSM) was generated. The algorithm was basically congruent with that used during the automatic tie point detection. Correlation is a frequently applied approach in photogrammetry for finding the common tie points of two images. Automatic DSM generation is achieved by a combined application of correlation calculations and tie point identification in digital photogrammetric software packages.

Using the query operator a series of feature points was determined on the images under study. Feature points are the center points of a window with acceptable greyscale and contrast values. Feature points on the other hand are also object points marking a single object, e.g. road crossing, bridge rail, monument etc. After the determination of interest points on a single image, the corresponding points are also identified in adjacent images, including the corresponding objects (Lee H. Y. et al. 2003). The next step is the calculation of cross-correlation between the sample window and the search window. The sample window is on the reference image, while the search window is on the adjacent image. As an interest point on the initial image might have several corresponding tie-points on the adjacent image, the program calculates a correlation coefficient for each suitable set of corresponding points. This coefficient expresses the rate of similarity between the corresponding interest points of the adjacent images. The higher the value the greater the similarity is (0.8-1).

Strategic parameters influence the success and accuracy of transformations. The most important parameters are those of the sample and search window sizes and the chosen correlation coefficient.

RESULTS

Accuracy assessment

A raster DSM image of 5 m grid size was created for the entire area (*Fig. 4*), an ESRI 3D shape file of ca. 450000 points. Furthermore, to set the most optimal program values a raster DSM of 2 m grid size was also generated for the south-east foothill area, and used for preliminary studies of the slopes with mass movements directed towards the Danube (*Figs. 5a-c*). In order to determine the exterior accuracy of the aerial triangulation and surface modelling methods, a new series of DGPS measurements is needed. Interior accuracy statistics might be helpful in the evaluation process. In the final solution every single tie points (GCP) had to be used due to the large spatial extent of the study area. In the iterative runs, a single GCP was left out and identified as verification point. The residuals received for these verification points always fell within the range of acceptable error in all three X, Y and Z directions as depicted on *Table 2.*

The calculated error values were compared to the exterior accuracy values of the known published studies. The verification results of two studies are depicted in *Table 3.* Altmaier A. and Kany C. (2002) used DGPS measurements to check the accuracy of 120 points, while Schenk T. et al. (2003) used 1:24000 topographic maps and 20 points to verify their results of image analysis. When we look at the findings of their and our studies we

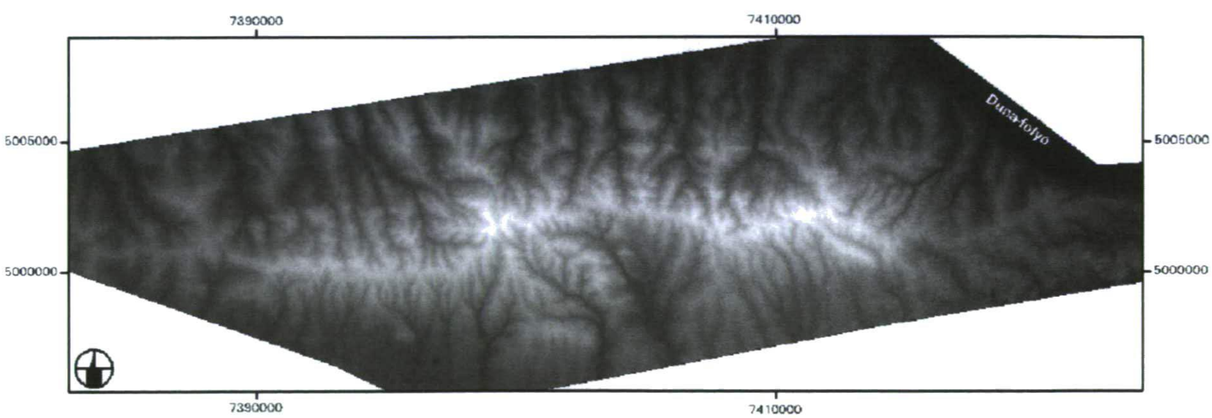

Fig. 4 A DSM of 5m grid size of the Fruška Gora (coordinate system: Gauss-Krüger, Yugoslavia)

can conclude that the digital photogrammetric analysis of CORONA KH-4A/B satellite images generally yield a vertical accuracy of 10-25 and a horizontal accuracy below 10 m. Considering the relatively low cost of images and the relatively large area covered by an image pair subjected to study, these findings are rather satisfying.

Table 2 Residuals received for aerial triangulation, DSM verification for the surficial interest points expressed in meters

	Aerial triangulation			*DSM img*	*DSM 3D shape*
	X	*Y*	*Z*	*DSM Z – GCP Z*	
minimum	0.6	4.4	3.4	2	5.3
maximum	15.5	12.9	24.9	25.1	27.1
average	6.7	8.0	8.6	10.7	13.7

Table 3 Collective results of accuracy studies in referred works (Altmaier A. – Kany C. 2002, Schenk T. et al. 2003)

	Average			
	X	*Y*	*Z*	*DSM Z – DGPS Z*
Aerial triangulation for two models (A. Altmaier)	2.5-4.8	2.7-5.7	12.5-21.6	-
Aerial triangulation (T. Schenk)	6.2	5.6	12.34	-
DSM (A. Altmaier)	-	-	-	9.7-13.3

Possibilities for spatial visualization and other uses

Using the oriented model and the gained DSM, an orthophoto of the study area was generated with a resolution of 2x2 m using the OrthoBase program. The raster DSM was used as an input into the ERDAS VirtualGIS module, orthophotos and other vector layers like contourlines were placed on the surface model. The DSM 3D shape points were evaluated using ERDAS Stereo Analyst module, using an anaglyph and real spatial visualization approach, and StereoEyes liquid crystal glasses.

The available vector overlays were applied on the DSM to check the real spatial orientation of the individual data points. 2D vectorial overlays can be easily transformed into 3D overlays in most 3D image processing systems. The attribute tables can be individually displayed and edited during the evaluation process.

The DSM of 2 m resolution is also applicable for geomorphological investigations. One cross-section was drawn according to DSM (*Fig. 6a-b*), which is comparable with other section drawn by Pécsi M. (1979) at Dunaföldvár (*Fig. 6c*) Hungary. Comparing this old section with new, field measurements it can be used for the calculation of speed of landslide processes.

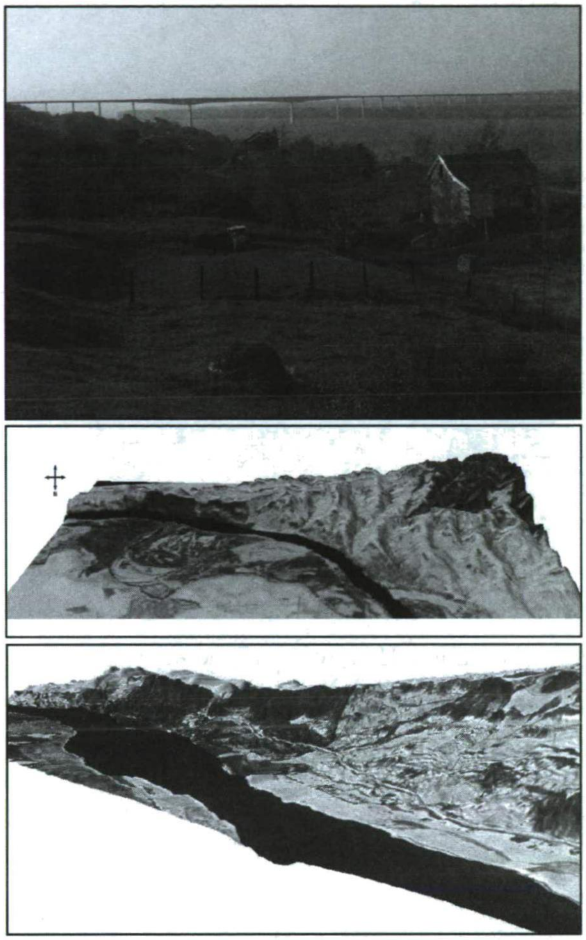

Figs. 5a-c A virtual image of the study area derived via the combination of an orthophoto and the DSM of 2 m grid size (photo: Mészáros M.)

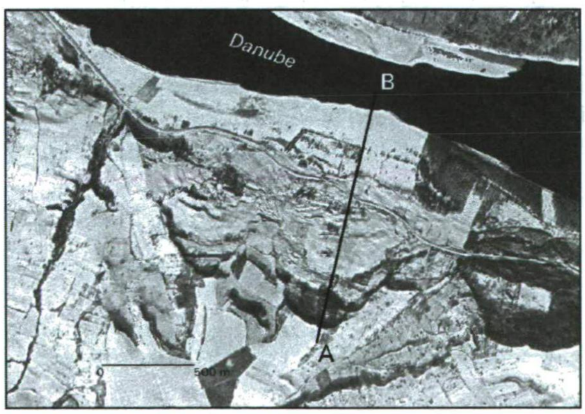

Fig.6a Landslides on the Corona image on the riverbank of Danube east to Fruška gora

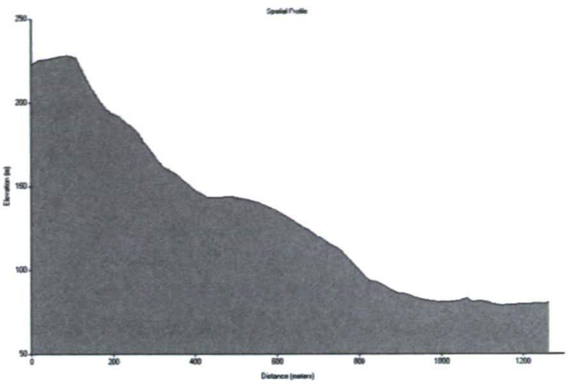

Fig. 6b Cross section of landslide marked on *Fig. 6a*

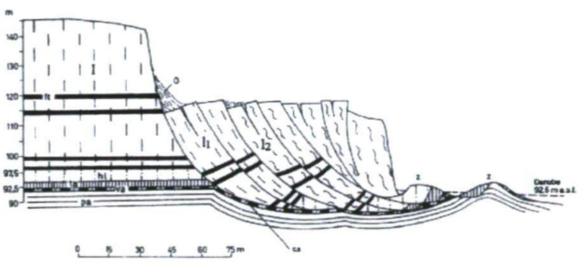

Fig. 6c The Dunaföldvár river-bank landslide to the S of the Danube's 1560 km mark (Pécsi M. et al. 1979)

l=loess sequence in primary position (autochtonous); l1=loess recently displaced by sliding; l2=waste of earlier slides; h1 pale pink sandy loess; o=talus; z=earth heap and Pannonian clay arising from the Danube's bed; fl=fossil soils; ta=dark grey clayey loam soil; pa=Pannonian clay; va=red clay, cs=sliding plane

SUMMARY

A DSM of the Fruška Gora was prepared using photogrammetric approaches and field GPS records. Corona stereo satellite images were not applied in Hungary before to create DSM. A raster type DSM image of 5 m grid size was created for the entire area, with an ESRI 3D shape file of ca. 450,000 points. Furthermore, to set the most optimal program values a raster type DSM of 2 m grid size was also generated for the north-east foothill area. The geometric resolution was adequate enough to visualize such geomorphological phenomena as land slides, erosion valley, etc.

References

Altmaier A. – Kany C. 2002. Digital surface model generation from CORONA satellite images. *ISPRS Journal of Photogrammetry & Remote Sensing* 56: 221-235

Bayram B. – Bayraktar H. – Helvaci C. – Acar U. 2004. Coastline change detection using Corona, SPOT and IRS 1D images. *International Archives of Photogrammetry and Remote Sensing* XXXV(B7): 437-441

Clinton W. T. 1995. Release of Imagery Acquired by Space-Based National Intelligence Reconnaissance Systems - Executive Order 12951 of February 22, 1995 *Federal Register* / Vol. 60, No. 39 / Tuesday, February 28, 1995 / Presidential Documents 10789-10790

Dashora A. – Lohani B. – Malik J. N. 2007. A repository of earth resource information - the Corona satellite programme. *Current Science* 92/7: 926-932

Lee H. Y. – Kim T. – Park W. – Lee H. K. 2003. Extraction of digital elevation models from satellite stereo images through stereo matching based on epipolarity and scene geometry. *Image and Vision Computing* 21/9: 789-796

Pécsi M. – Scheuer Gy – Schweitzer F. 1979. Engineering geological and geomorpholigical investigation of landslides in the loess bluff along the Danube in the Great Hungarian Plain. *Acta Geologica Acad. Sci. Hung.* 22/1-4: 345-355

Pécsi M. 1991. Geomorfológia és domborzatminősítés, MTA Budapest: MTA. 296 p.

Schenk T. – Csatho B. – Shin S. W. 2003. Rigorous panoramic camera model for disp imagery. ISPRS Hannover Workshop In proceedings of ISPRS Hannover Workshop 2003 www.ipi.uni-hannover.de/fileadmin/institut/pdf/schenk.pdf

Timár G. – Molnár G. – Pásztor Sz. 2002. A WGS84 és HD72 alapfelületek közötti transzformáció Molodensky-Badekas-féle (3 paraméteres) meghatározása a gyakorlat számára. *Geodézia és Kartográfia* 54/1: 11-16

Timár G. – Aunap R. – Molnár G. 2004. Datum transformation parameters between the historical and modern Estonian geodetic networks. *Estonia Geographical Studies* 9: 99-106

Journal of Env. Geogr. Vol. I. No. 1-2. pp. 11-21

PHYSICAL, CHEMICAL AND BIOLOGICAL ASPECTS OF HUMAN IMPACTS ON URBAN SOILS OF SZEGED (SE HUNGARY)

Puskás, I.[1] – Prazsák, I.[2] – Farsang, A.[1] – Maróy, P.[2]

[1] Department of Physical Geography and Geoinformatics, University of Szeged, P.O. Box 653, Szeged H-6720, Hungary
[2] Department of Genetics, University of Szeged, Közép fasor 52., Szeged H-6725, Hungary

Abstract

Urban soils have generally suffered significant alteration both regarding their physical, chemical, as well as biological properties. Soil samples were taken at 25 sites from horizons of soil profiles located in the downtown and surroundings of Szeged in order to examine diagnostic properties different from natural soils (artefacts, humus content, quality of organic matter, pH (H_2O, KCl), carbonate content, nitrogen content). Furthermore, topsoils were taken nearby 9 profiles to survey some basic biological properties (i.e. abundance, taxon diversity, dominance, similarity and MGP ratios) of mezofauna elements (Oribatid mites, Collembolans) and their community structure in the three zones (city, suburban, peripheral). The high amount of artefacts, fluctuating humus and nitrogen levels, the poor quality of organic matter, the high and fluctuating carbonate content, the concomitant variance of pH and modified mechanical properties prove that the urban soils of Szeged have been modified by anthropogenic activities. Surprisingly, it seems that the intermediate suburban zone has a more heterogeneous and stable mezofaunal community structure than the other two.

Key words: urban soils, diagnostic properties, Collembolans and Oribatid mites in soils

INTRODUCTION

Urbanization results functional and qualitative changes in natural ecosystems, and alters the ecological balance. Urban ecosystems are heterogeneous formations in which soils, flora and fauna are considerably transformed due to anthropogenic pressure. Urban soils attract more and more attention, as they are one of the key elements of urban ecosystem (Beyer L. et al. 1995). The determination of their properties is of great importance both from the aspect of soil science and human health (Simpson T. 1996). Urban soils are very diverse since on one hand they have characteristics close to those of natural soils, on the other hand they are the result of human activity. Consequently, their physical and chemical properties have suffered significant alteration in contrast to natural soils in the surroundings of human settlements. The specific characteristics of these soils are high alkalinity, stratification, clear evidence of technogenic impacts, soil surface sealing, compaction, mixing of anthropogenic (e.g., brick and mortar debris, garbage, rubble, ashes) and natural materials and an increased content of nutrients and toxic elements (Schleuss U. et al. 1998). Therefore, the original multifunctional character of urban soils is gradually lost, they are no longer capable to fully fulfill the functions of natural soils (Stefanovits P. et al. 1999). On the other hand, the weakening and finally the loss of the original functions opens up the way for the development of new special functions, as the city generally hosts a wide range of human objects (building, parks etc.) and activities (transportation, industrial production, trade, waste management and disposal etc.).

The modified physical and chemical parameters exert an influence on soil organisms. As a result, the biological properties of urban soils also differ from those characterising other managed and natural systems (White C. S. – McDonnell M. J. 1988). A general demand of soil research is to evaluate the effect of human activity by applying biological indicators, as physical and chemical parameters cannot completely describe the quality of urban soil. The study of microarthropod communities (besides microfungi and bacteria) can be a powerful method for assessing soil quality because life cycles of these edaphic animals strictly depend on soil characteristics. In terrestrial ecosystems Oribatid mites and Collembolans are represented by the number of species (Stanton N. L. 1979). They generally account for up to 95% of total the number of microarthropods in grassland and play an important role in decomposing organic materials changing the physical and chemical texture of soils, cycling nutrients, and conserving soil environment (Wallwork J. A. 1983). The close relationship between edaphic invertebrates and their ecological niches in the soil, and the fact that many of them live a rather sedentary life provide a good base for the bioindication of changes in soil properties and the extent of human impact (van Straalen N. M. 1998). In all, Collembolans and Oribatid mites are excellent means for assessing and monitoring soil quality and predicting activity of the soil processes, especially those which occur due to human intervention.

After considering the above-mentioned facts, the major aims of the present study can be summed up as follows:

- to examine the physical and chemical properties different from those of natural soils (e.g. artefacts, organic matter content, quality of organic matter, pH

(H_2O, KCl), carbonate content, nitrogen content, total salt)

- to survey the mezofauna (Oribatid mites, Collembola) of different urban soils

STUDY AREA, MATERIALS AND METHODS

Szeged is a major city with the lowest elevation of 84 m ASL in Hungary. The surface is prevailed by elements of the fluvial systems of the rivers Tisza and Maros composed of active and inactive channels (Marosi S. – Somogyi S. 1990). After the Great Flood of 1879 two major flood protection systems were devised: one was relying on the newly constructed ring of dams embracing the inner core areas, the other is based on an elevation of the original surface via significant infilling of the low-lying areas. The largest thickness of the infill, exceeding 6 m, is recorded in the downtown area in the vicinity of the downtown bridge (Andó M. 1979).

Anthropogenic soil evolution was initiated in the city of Szeged on the following natural soil types: on the right banks of the river Tisza west and north-west of the city high quality Phaeozems developed on a loessy bedrock. The highly compact alluvial bedrock of the region of Újszeged favored the evolution of Fluvisols with different degree of maturity. The southern areas of the city are covered by Gleyosols. While the areas just north-east of Szeged are covered by highly compact Solonetz soils of poor hydrological parameters.

Samples were taken at 25 sites from the identified horizons of the individual soil profiles yielding a total of 127 samples for further study (*Fig. 1, Table 1*). The samples were dried, crushed and sieved through a mesh of 2 mm for further analysis. The artefact content was determined by giving the m/m % of the fraction remaining on the sieve. The pH (H_2O, KCl) was recorded using a digital pH measuring device of Radelkis type. In order to capture the hidden acidity of soils the pH of a KCl soil suspension was also recorded. The organic content was measured after H_2SO_4 digestion in the presence of 0.33 M $K_2Cr_2O_7$. The quality of humus was given by the humus stability coefficient (K value). The total salt content of the soils was determined via recording the electric conductivity of fully saturated soil samples. The carbonate content of dry soil samples given in percentage was determined via Scheibler-type calcimetry. The nitrogen content was measured using nitrogen distilling device type Gerhardt Vapodest 20. The mechanical composition was determined by the yarn test of Arany (Buzás I. et al. 1988).

According to the investigations of Szemerey (2004), the presence of the mezofauna in the soil is the greatest during spring and autumn. Consequently, soil samples were taken in October 2006, nearby 9 profiles (No. 1, 2, 4, 9, 11, 15, 16, 18, 22), representing three zones (city,

Fig. 1 Location of sampling sites on a map of the city of Szeged

Table 1 Characteristics of the sample sites

Profiles	*No. of soil horizons*	*Bedrock*	*Morphology*	*Perched groundwater depth (cm)*	*Landuse (2005)*	*Vegetation cover (2005)*
1.	6	infill	plain	> 200	Built-in area	-
2.	4	loess	plain	> 75	Meadow	Lolium perenne, Taraxacum officinale
3.	9	loess	plain	> 125	Bicycle road	Taraxacum officinale, Elymus repens, Lolium perenne,
4.	6	infill	depression	> 80	Abandoned area	Rosa canina, Phragmites australis, Poa trivialis, Arrhenatherum elatius
5.	5	infill	plain	> 140	Sidewalk	-
6.	6	infill	plain	> 150	Built-in area	Elymus repens, Ambrosia artemisiifolia, Erigeron canadensis, Chenopodium album,
7.	4	loess	plain	> 180	Built-in area	-
8.	8	infill	slope	> 180	Meadow	Taraxacum officinale, Elymus repens
9.	4	infill	plain	> 155	Built-in area	-
10.	5	mud	plain	> 180	Built-in area	-
11.	6	infill	plain	> 180	Built-in area	-
12.	7	loess	plain	150	Plot	Ambrosia artemisiifolia, Elymus repens, Polygonum aviculare
13.	5	infill	plain	> 150	Built-in area	-
14.	5	loess	plain	> 170	Common	Artemisia vulgaris, Cichorium intybus, Achillea millefolium
15.	8	loess	plain	> 200	Dirt road	Cichorium intybus, Taraxacum officinale
16.	3	loess	plain	>130	Arable land	Daucus carota, Petroselium crispum
17.	3	loess	plain	>95	Arable land	Medicago sativa
18.	2	mud	depression	80	Meadow	Lythrum salicaria, Bolboschoenus maritimus, Carex vulpina
19.	2	mud	depression	50	Arable land	Zea mays
20.	5	loess	plain	>135	Orchard	Brassica oleracea, Pisum sativum
21.	4	loess	plain	100	Orchard	Solanum lycopersicum, Capsicum anruum
22.	10	infill	plain	>180	Park	Taraxacum officinale, Lolium perenne
23.	4	loess	plain	>120	Orchard	Brassica oleracea, Allium cepa
24.	3	mud	plain	>85	Pasture	Festuca pseudovina, Artemisia santonicum, Limonium gmelini
25.	3	mud	depression	>80	Pasture	Potentilla reptans, Phragmites australis

suburban, peripheral zone). One sample (No. 26) was not originating from the close vicinity of a profile, but it was taken from under a peripheral zone deciduous forest. For the analysis of the soil fauna top soil (0-5cm) samples were applied, which were gained from two 30x30cm quadrates. The extraction of the tiny soil microarthropods in isopropyl-alcohol was carried out using a modified Balogh extractor within 5-6 hours after sample collection (Hoblyák J. 1978). The samples were treated with saturated NaCl suspension (Móczár L. 1962.) and filtered with vacuum sieve. The extracted animals were sorted under a binocular stereomicroscope. Adult Oribatid mites were identified in lactic acid to a genus level, and if it was possible species were also determined, using 100x, 200 x magnifications. The taxonomy of Oribatid mites is well studied, thus the identification of genera can be made confidently with the available identification books (Balogh J. – Mahunka S. 1980, Balogh J. – Balogh P. 1992, Weigmann G. 2006). The Collembolans were identified to families under binocular stereomicroscope following Bellinger's online identification database (1996-2007) and Bährmann's identification book (Bährmann R. 2000). The community structure of Oribatid mites was determined on the basis of *abundance*. Abundance stands for the number of adult individuals in each taxa, and it provides data on the distribution of mites in a given amount of soil sample. Nymphas were not counted since their identification has not been clearly defined yet.

The *diversity* of mesofaunal communities was also determined, meaning that the number of taxa (genera) was counted in a given amount of soil sample. The structure of Oribatid mite communities was described with the *genus dominance index,* calculated with the help of the following formula (Hoblyák J. 1978):

$$D= s/S*100$$

(s: The number of individuals belonging to a given genus in the sample; S: The summed number of individuals of all genera in the sample)

To compare the genus composition of Oribatid mite communities, located in the city, suburban and peripheral zones, *the Sørensen index* was used (Mátyás C. 1996). The value of the index ranges between 0 and 1, depending on the presence of common taxa (here genera).

$$Cs=2*c/(A+B)$$

(c: the number of common genera; A, B: all genera in the given samples)

Furthermore, an MGP analysis was also applied in order to evaluate the stability of the Oribatid mite community in the 3 urban zones. This method is based on the proportion of the three major taxonomic units (Macropylina: M, Gymnonota: G and Poronota: P) (Balogh J. 1972). All of the three major taxonomic units have distinct ecomorphological features and their proportion is different at the various stages of association development (Aoki J. 1983). The criteria for the establishment of MGP types are as follows:

- >50% individual number of Macropylina to total individual number (or total species number)→ M type
- >50% individual number of Gymnonota to total individual number (or total species number)→ G type
- >50% individual number of Poronota to total individual number (or total species number)→ P type
- >20% and <50% of each 3 groups to total individual number (or total species number)→ O type
- >20% and <50% of each M and G groups, and <20% of P group to total individual number (or total species number)→ MG type
- >20% and <50% of each M and P groups, and <20% of G group to total individual number (or total species number)→ MP type
- >20% and <50% of each G and P groups, and <20% of M group to total individual number (or total species number)→ GP type

The MGP-I analysis is based on the number of species, whereas the MGP-II is based on the number of individuals using the above criteria. Collembolans were classified into 4 superfamilies each corresponding to a major ecomorphological group (Parisi V. et al. 2003). The abundance of each superfamily was determined in the three different urban zones.

RESULTS AND DISCUSSION

Evaluation of physical and chemical properties

First of all, those physical, chemical properties of Szeged soils were examined, which can indicate human impact. The examined properties were chosen from the diagnostic properties of urban soils given by Hollis (1992). The main question was whether these physical and chemical properties were able to indicate urban influence on the soils of Szeged. On the other hand, we also assessed the degree and way, how the good indicators reflect the anthropogenic effects on urban soils.

The average *artefact content* of soil profiles ranged between 0.0-23.7%, with a minimum value of 0.0%, and a maximum value of 63.0%. 11 out of 25 profiles contained no artefact at all. Some of these profiles (No. 16, 17, 18, 19, 24, 25), originating from the most peripheral parts of the city, represented original genetic soil types, thus the lack of artefacts was due to insignificant urban activity. This parameter was not present in further 3 profiles, originating from small orchards situated on the outskirts (No. 20, 21, 23). Profiles with very few (0-2%) or few artefacts (2-5%) were either found in the surroundings of the city, where the thickness of the infill is relatively negligible (profiles No. 10, 12, 14, 15); or in the downtown where the infill might be considerable, but of higher quality and lack of artefacts (profiles 1, 5, 13). To the category common (5-15%) the profiles (No. 3, 8, 9, 11) with either partly or fully containing infill can be placed. Profiles containing a large amount of artefact (15-40%) were entirely composed of artificial infill. Thus, the minimum, maximum values and the standard deviations were also striking in case of these profiles (No. 4, 6, 22). Consequently, the amount of artefacts is not decreasing towards the city margins, because this property changes rather due to "point" factors and not regional ones (FAO 2006).

The *mechanical soil types* of Fluvisol, Gleyosol, Solonetz soils are clay, heavy clay, whereas in case of Phaeozem soil type clayey mud is typical. In some profiles (No. 7, 14), located in the surroundings of the city, the original soil horizons could remain. Towards the margins of the town, mixed profiles (No. 2, 3, 8, 12, 15), composed of landfill and original buried soil horizons, were also found. The horizons representing infill were dominated by sand, sandy mud and mud, while those preserving the original conditions by clayey mud. In the profiles composed of purely artificial infill (No. 1, 4, 6, 9, 11, 22) also sand, sandy mud and mud were dominant. The abrupt textural change was mostly characteristic of artificial horizons in contrast to the gradual textural change of natural horizons. This is also an excellent indicator of human influence.

The average *humus content* of the profiles was between 0.6 and 2.3%, with a maximum of 3.7% and a minimum of 0.0%. If considering the average values, only one profile (No. 18) developed on a natural Gleyosol, showed normal humus content (2-4%). Certain profiles were classified into the category of extremely poor humus content (<1%), while the majority fell into the category of poor humus content (1-2%). To the category extremely poor profiles No. 1 and 5 with fully containing infill in the downtown area and the profiles (No.

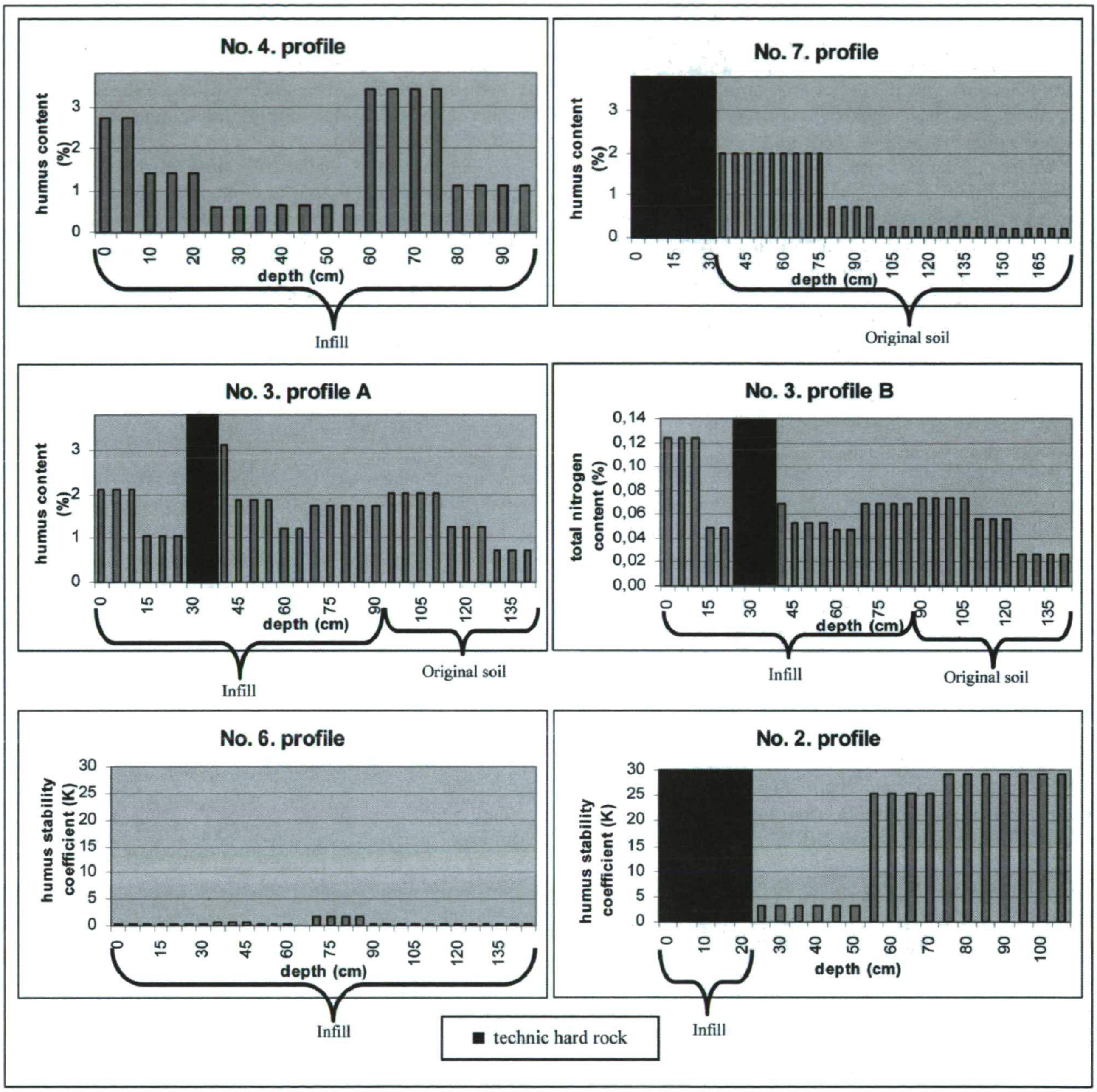

Fig. 2 The humus content and nitrogen content of some studied profiles

2, 7, 12, 14) with slight amount of infill on outskirts can be placed. The remaining 17 natural and artificial profiles fell into the category of poor humus content. It might be more important to study the distribution of this parameter along individual profiles, as it can clearly show the degree of human impact. Along a natural profile, humus content is congruent with original genetic soil type: it shows generally gradual downward decrease towards the bedrock (Lorenz K. – Kandeler E. 2005) (*Fig. 2*, profile No. 7). Conversely, the humus content tends to display an irregular fluctuation in those profiles which are fully made up of artificial infill, depending on the humus content of the layers utilized (*Fig. 2*, profile No. 4). However, we also found mixed profiles embedding considerable amount of infill material and buried soil horizons as well. In case of these latter ones, the tendency for the humus content is congruent with that of natural soils from the appearance of the A horizon of the original buried soil (*Fig. 2*, profile No. 3/A).

The significant alteration of physical, chemical and biological properties of urban soils influences the nitrogen cycle of these soils (Beyer L. et al. 1995, Craul P. J. 1999). Thus, besides the determination of humus content as a complementary analysis the *total nitrogen content* of the soil samples was also measured. The average nitrogen content of the profiles was between 0.02 and 0.11%, with a maximum of 0.19% and a minimum of 0.0%. The amount of nitrogen in soils is primarily determined by the type and intensity of microbial activities. Consequently, the highest nitrogen values are recorded in those horizons where biological activity is the strongest and the largest amount of humus is produced (Stefanovits P. et al. 1999). As a matter of fact, the distribution of nitrogen along the studied profiles showed similar tendencies as in the case of humus. Thus, infilled horizons represented fluctuating nitrogen content, while natural horizons corresponded to the characteristic of the genetic soil types (*Fig. 2*, profile No. 3/B). Beside the distribution of nitrogen along a profile, it is also important to evaluate quantitative differences: most profiles fell into the category of extremely poor nitrogen content (<0,05%), profiles with higher amount of humus were classified into the category of poor nitrogen content (0,05-0,10%).

From the practical side it is important to know the ratio of well-humified, condense humus components composed of larger molecules, serving as primary agents in establishing the structure of the soil as well as its nutrition content, to those organic components which are not bond to calcium and less humified. This ratio is clearly depicted by the *K value*. The average K values were between 0.3-14.4 with a minimum of 0.0, a maximum of 29.2, indicating significant differences among profiles. Since the urban soils in the downtown of Szeged are "young" soils in contrast to the natural soils in the surroundings of the city, they have not had enough time for the formation of good quality humus yet. Consequently, the horizons with considerable amount of artificial infill were characterized by very low K values, indicating the prevalence of raw humus components, i.e. fulvic acids not yet subjected to humification (*Fig. 2*, profile No. 6). However, those mixed profiles containing remains of the original natural soil horizons as well had higher K values referring to the dominance of high-quality humic acids in these levels (*Fig. 2*, profile No. 2).

The average *carbonate content* of soil profiles ranged between 0.9-25.6%, with a minimum value of 0.08% and a maximum value of 40.2%. Considering the profile average values, one can be placed into the category extremely calcareous (>25%). Thirteen heterogonous profiles can be classified into the category highly calcareous (10-25%). Profile No. 17, representing this type, is located in the surroundings of the city on Phaeozem as original genetic soil type. Profiles No. 20 and 21 are located in orchards of the outskirts and developed on Phaeozem soils free of infill. In case of some further profiles (e.g. profiles No. 7, 12, 14) of highly calcareous character the loessy bedrock was the most important source of the high carbonate content.

These profiles are located in the suburban area, in surroundings of the city on a Phaeozem and represent a mixture of natural soil horizons and artificial infill. In such profiles there was a gradual downward increase in the carbonate content towards the bedrock from the first natural soil horizon (*Fig. 3*, profile No. 12). The reason for this is the leaching of carbonate phases from the upper soil horizons and the accumulation of these in the underlying layers or the bedrock itself. The other remaining half of the highly calcareous profiles were composed of fully artificial infill. Here either the considerable amount of carbonate-rich artefacts or the carbonate rich infill horizons were responsible (*Fig. 3*, profile No. 1). On the other hand, some profiles (No. 8, 9, 11, 13) containing artificial infill could still have lower carbonate content. These and the natural profiles (e.g. No. 16, 18, 19, 24) with relatively lower carbonate values formed the category of moderately calcareous soils (2-10%). Two profiles representing Fluvisol fell into the

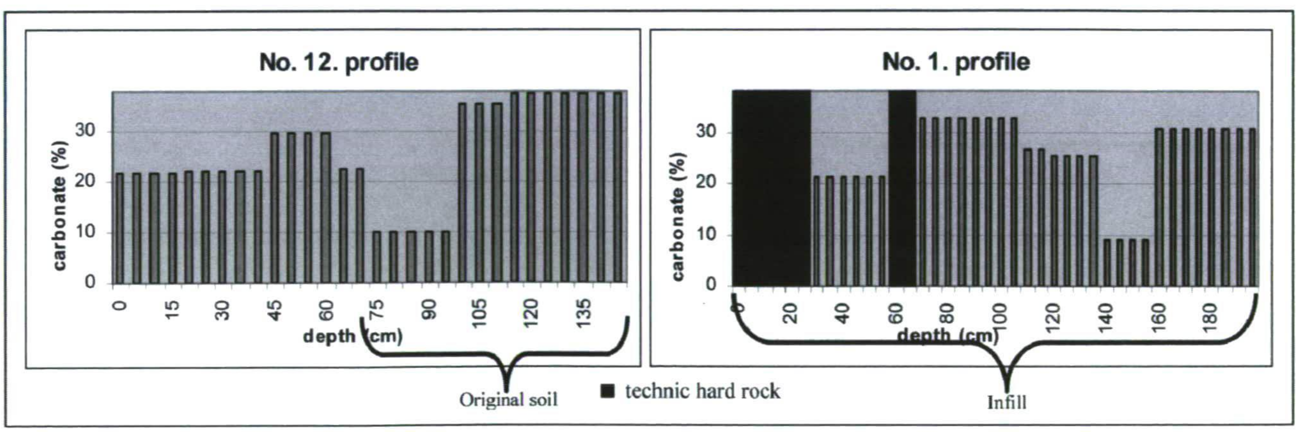

Fig. 3 The carbonate content of some studied profiles

Table 2 The dominant and characteristic genera of Oribatid mites at different urban zones. (Those genera are presented the proportion of which was above 10%)

Urban zone	*City*				*Suburban*			*Natural*		
Sample No.	*1*	*11*	*9*	*22*	*2*	*4*	*15*	*18*	*16*	*19*
Dominant genus	Rhysotritia 40.7%			Rhysotritia 90%	Tectocepheus 60%	Rhysotritia 41%	Zygoribatula 51.5%	Tectocepheus 17.4%	Eupelops 67.5%	Tectocepheus 60.8%
Characteristic genus	Scheloribates 34.6					Scheloribates 33%	Ceratozetes 28.1%	Eupelops 12.9%	Tectocepheus 31.1%	

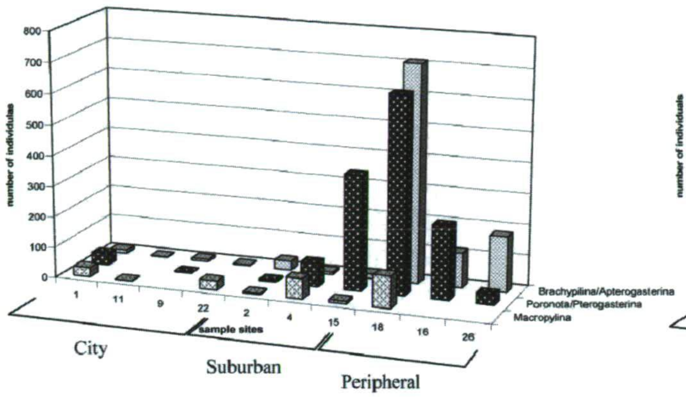

Fig. 4 The number of oribatid mites for major taxonomic groups at each sample site

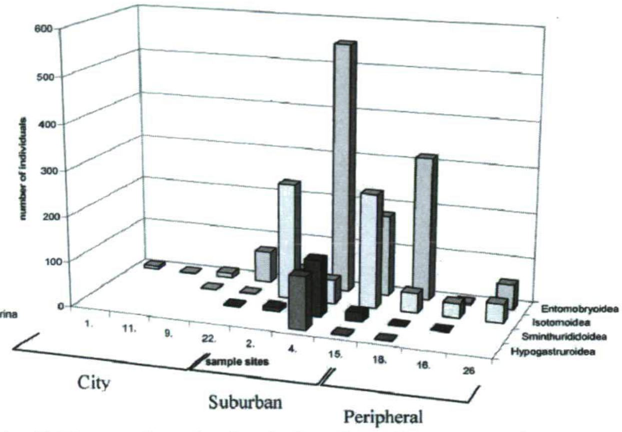

Fig. 5 The number of collembolans for major taxonomic groups at each sample site

category of slightly calcareous soils (0-2%). As a result of regular flooding, only the uppermost horizons of these profiles contained aerated carbonate (FAO, 2006).

The averages of the *pH(H_2O)* were between 7.7-9.7 with a minimum of 7.3, a maximum of 10.0. The *pH(KCl)* averages were between 6.9 and 8.7, with a minimum of 6.7, a maximum of 9.0. Based on average values of the pH(H_2O), only profile No. 24 was classified into the category of strongly alkalescent soil. All other profiles fell on the transitional line between categories of slightly alkaline and alkaline soils. The close correlation between recorded pH values and carbonate content is rather obvious: the high carbonate content results in high pH values. Thus, observed fluctuations of the carbonate content within the studied profiles were congruent with the pattern observed in the pH values. Those profiles were alkaline which were located on Phaeozem containing infill material with considerable carbonate content and buried soil horizons with very significant carbonate content. The loessy bedrock of buried soils could increase further the pH average.

Investigation of mezofauna (Oribatid mites and Collembolans)

The concept that the higher soil quality is the more microarthropod groups identified had been proposed (Parisi V. et al. 2003), and even it was formulated as QBS (i.e. "Qualità Biologica del Suolo", namely Biological Quality of Soil). We followed this concept in the case of our study, except for the fact that we analysed only the most abundant mezofaunal elements: Oribatida („box mites") and Collembola (springtails). Statistical analysis was omitted, since it requires repeated samplings for at least 1-2 years. The gained results provide a rapid and robust tool for soil science to evaluate the biological activity of urban soils. Oribatid mites and Collembolans were found at each sampling point, but the numbers of individuals belonging to the different taxa were very different.

The collected 2744 adult Oribatid mites belonged to 54 taxa. 40 of the 54 taxa were identified to species and 14 to genus level. Approximately 10% of the Hungarian Oribatid fauna were recorded in the samples of Szeged and its peripheral belt. This number, compared to the values of a natural deciduous forest, rich in Oribatid mites, is not too low. Macropylina, Brachypilina (Gymnonota) and Brachypilina (Poronota) gave 12.9%, 40.7% and 46.4% of the identified adult mites, respectively.

In the *city zone* 8 genera were found, all with a very low abundance (52 sp./m^2). The number of city zone genera was only 15% of the total genus number found in this study. Although this zone is the most disturbed and polluted, a very rare Mediterranean species (*Lohmannia turcmenica*, Bulanova-Zachvatkina, 1960), a special wetsoil mite (*Scapheremaeus palustris*, Sellnick, 1924) and a yet undefined Oppiinae species were found here.

These rare species did not appear at other parts of the study area. Due to the low number of specimens, only two samples (No. 1, 22) were suitable for calculating the dominance index. In this zone Rhysotritia was the absolute dominant (90% and 40.7%) and Scheloribates was the characteristic genus (*Table 2*).

The *suburban zone* was unambiguously different in terms of specimen density and taxon diversity (*Fig. 4*). Compared to the city zone in this intermediate or transitional area twice as many genera (20) were identified, and the values of abundance were an order of magnitude higher (657 sp./m^2). The sites in this zone community structure of Oribatid mites were very heterogeneous. Heterogeneity is well signed by the fact that each site differed in terms of both the dominant and characteristic genera (*Table 2*). Community struc-tures indicate a transition between those of the city and the peripheral zone. This is also suggested by the fact that both the typical genera of the city and the peripheral zone were represented here by high individual numbers. Towards the peripheral zone taxon diversity gradually increased (*Fig. 6*). Members of the Macropylina group (Rhysotritia, Eniochthonius, Nothrus) appear with relatively high individual numbers, and different kinds of Zygoribatula and Oppiidae (Dissorrhina, Neotrichoppia, Oppiella, Oppia, Ramusella) genera did also occur. The number of genera (Eniochthonius, Belba, Dorycranosus, Suctobelba) recorded exclusively in this zone was nearly as much as in the peripheral zone.

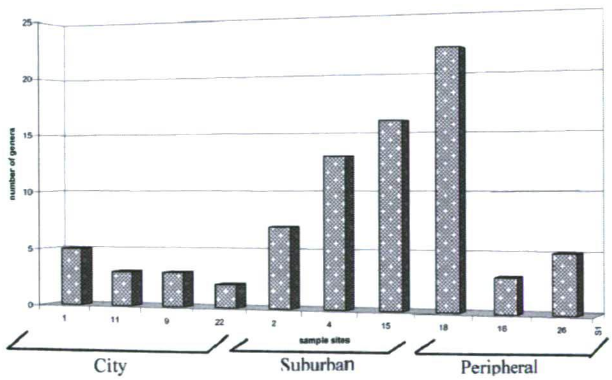

Fig. 6 The number of genera of Oribatid mites at each sample

The Oribatid mite density in the *peripheral zone* with close to natural habitats was much higher than in the former zones. In fact, it is an order of magnitude higher (2252 sp. /m^2) than the density determined in the suburban zone. This zone had the highest number of taxa, 44% of the total genus number. However, this is not a dramatic difference compared to the suburban zone. The highest number of individuals, 53% of the total number, was also identified here.

It is well visible on *Fig. 4* that the 3 peripheral zone sites showed great heterogeneity both in terms of specimen number and community structure. Note that the abundance and heterogeneity indices of sample No. 16 and 26 were significantly lower than those of sample No. 18. Soil type, the absence of vegetation cover and the type of agricultural cultivation could be responsible for the development of the poor community structure similar to those in the city. In case of sampling site No. 16 perhaps low moisture content of the sandy topsoil and sparse vegetation cover provided unfavourable conditions for Oribatid mites. On the contrary, the dense vegetation cover at sample No. 18 was much more preferable for these animals. Nevertheless, samples of this zone having lower genus number were still more diverse in terms of Poronota and Brachypilina (Poronota) groups than any other city zone samples. Depending on the type of habitat Eupelops and Tectocepheus were the dominant genera (*Table 2*).

The similarity analysis based on the Sørensen index showed that there were more common genera in terms of the suburban and the peripheral zone (C_S=0.50) than in case the city and the suburban (C_S=0.34) or the city and the peripheral (C_S=0.26) zones. All of these reflect the extreme character of city zone. The results of MGP-I and MGP-II analyses can be seen on *Fig. 7* and *8*. According to the MGP-I analysis, the patterns of the peripheral and suburban zones were similar, while that of the city zone differed from both. The genera based M:G:P ratio was 1:2:1 in the city and 1:2:2 in both the intermediate and peripheral zone (*Fig. 7*). In general, the intermediate and peripheral zones were GP-type, while the city zone was O-type. According to the MGP-II analysis, the above ratio was 1:1:1; 1:8:1 and 1:4:4 in the city, suburban and peripheral zones, respectively (*Fig. 8*).

Surprisingly, the proportion of M and G groups was relatively high in the city zone. Previously, such community structure was primarily found in stable closed canopy forests (Aoki J. 1983). However, due to low density values the above proportions have to be handled with care. The abundance and proportion of group G in the intermediate zone turned to be very high during the MGP-II analysis, this zone was characterized thus as G-type. The pattern of the peripheral zone was similar to the results received during the MGP-I analysis, so this area can be considered GP-type.

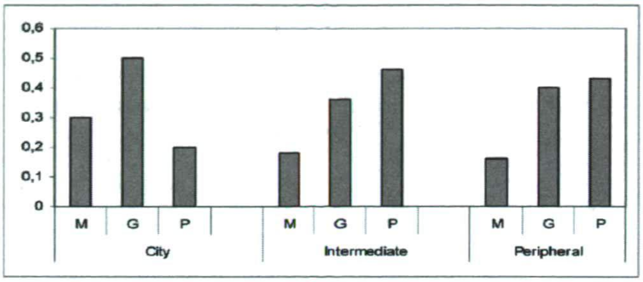

Fig. 7 MGP-I analysis: MGP ratios in the 3 different zones, based on number of genera

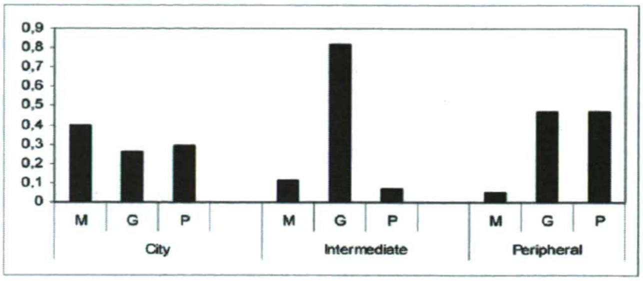

Fig. 8 MGP-II analysis: MGP ratios in the 3 different zones, based on the number of individuals

Our results from the city zone seemingly contradict the hypothesis described by Lee et al. (1999). According to their theory, the M:G proportion of Oribatid mites is considerably lower in a city environment than in close to natural areas, while the high proportion of the P group is due to the fact that its members are previously described as pioneer species. One of the reasons in the background of our different results could be the low number of individuals in the city zone, which might provide a distorted view on proportional values. Besides, the *Rhysotritia ardua* (member of the special group of Ptychoid within Macropylina) seemed to be more sensitive than it had been expected before the MGP analysis. Thus, in accordance with the opinion of its author, the MGP method requires further elaboration to provide a precise tool for the ecomorphological classification of Oribatid mites. 2063 Collembolan individuals were identified and classified into 4 superfamilies: Entomobryoidea, Isotomoidea, Sminthuridoidea, Hypogastruroidea. Most of Collembolans represented the Entomobryoidea superfamily, the second most abundant group was Isotomoidea with almost third of the total individual number (*Fig. 9*). The two remaining groups had low representation, and altogether gave 13% of the total number. 77% of the Collembolans originated from sampling sites of the suburban zone. The peripheral and city zone provided only 18% and 5% of the Collembolans, respectively. The suburban zone was especially interesting as each ecomorphological group had the highest individual number here (*Fig. 5*). Note that the Entomobryoidea group was much more common than the others, since its members were identified at all sampling sites. The most sensitive group was Hypogastruroidea, the members of which were collected in large numbers only in the suburban zone (sample No. 4). The presence of all the four ecomorphological groups signed higher diversity, which referred to less disturbance in this zone. Before the mezofauna investigation our basic hypothesis was that the number and abundance of taxa would increase from the city towards the semi-natural habitats of the peripheral zone. In accordance with the above, the lowest abundance values were experienced in the city zone, being an order of magnitude lower than elsewhere. There was a great difference between the taxon diversity of Oribatid mites in the city and the suburban zone, while the taxon diversity in the suburban and peripheral zones was similar. The low abundance in the city can be related to high air and soil pollution, habitat isolation and low moisture content of the soil (Weigmann G. – Kratz W. 1986). However, the mezofauna in the more polluted and disturbed habitats of cities are obviously more random (Erhard C. – Szeptycki A. 2002). That could be the reason for finding 3 peculiar species in the city zone of Szeged. The diversity of dominant species was the greatest in the suburban zone. This fact and high individual numbers suggest that the intermediate zone is a relatively good habitat. Based on the dominant Oribatid mite species of the suburban zone, the transition between the barren city and heterogonous peripheral zones could be considered continuous. The high individual and genus number of Gymnonota and Poronota taxa in the suburban and peripheral zones suggested a more stable Oribatid mite community. The abundance pattern of Collembolans corresponded well to that of Oribatid mites. The diversity and abundance of Collembolans were the lowest in the city zone. It seems as if Collembolans accumulate rather in suburban soils in contrast to Oribatid mites, which are more abundant in peripheral soils.

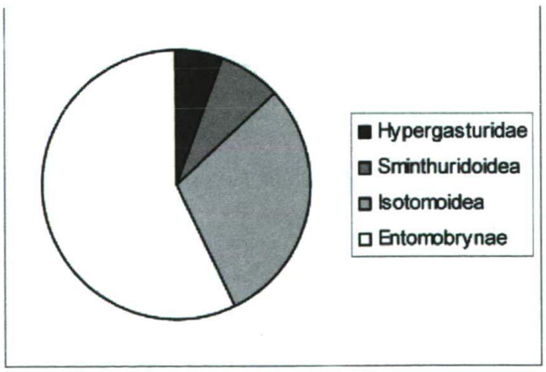

Fig. 9 Proportion of the major Collembolan groups of all samples

CONCLUSION

All the soil parameters mentioned so far are excellent markers of human influence in urban soils. This can be seen either in a change in their recorded concentration values or the alteration of their vertical distribution in the profiles. An elevated amount of artefacts, the fluctuating humus and nitrogen levels, the poor quality of the humic material, the high and fluctuating carbonate content and a concomitant variance in the pH, the modified mechanical properties all refer to a soil affected and transformed by human activities.

Beside the physical and chemical properties of the soil, the biological indicators were also analyzed. The diversity of soil mezofauna communities was expressed with "genus diversity". To analyze the similarity of Oribatid mite genus composition between two urban regions the Sørensen index was applied (Mátyás C. 1996). Identifications to more general levels can be declared an efficient way of assessing biodiversity rapidly and it is therefore likely to be used by land-use planners and urban environmental consultants who are concerned with the rapid changes in the biota as a result of urbanization (Mclntyreet N. E. et al. 2001, Parisi V. et al. 2003). For that reason, we have identified the selected groups to family and genus level. Our results greatly support those of a former investigation by Magura T. et al. (2006) in which they found that intermediate, transitional areas between the city and the peripheries show a greater diversity than the later two. It seems that this intermediate zone is stable and heterogeneous enough to constantly provide the species for the city and peripheral areas. The concentric structure of Szeged is also important in ensuring a gradual transition between the city and the peripheral areas. Since there is no contiguous industrial zone, the intermediate area between the city and the peripheries can be a significant buffer and refugium for soil microarthropods.

Acknowledgement

We would like to express our appreciation to all those who contributed to our work. Ibolya Tápai chemical assistant and István Fekete chemist working for our department (Department of Physical Geography and Geoinformatics, University of Szeged) gave useful comments for the chemical analysis. Finally, authors wish to thank to Zoltán Winter for his help in preparing the figures.

References

Andó M. 1979. Szeged város település-szintje és változásai az 1879. évi árvízkatasztrófát követő újjáépítés után. *Hidrológiai Közlöny* 6: 274-276

Aoki J. 1983. Analysis of Oribatid Communities by Relative Abundance in the Species and Individual Numbers of the Three Major Groups (MGP-Analysis). *Bulletin of Institute of Environmental Science and Technology* 10: 171-176.

Balogh J. 1972. The Oribatid Genera of the World. Budapest: Akadémiai Kiadó. 31 p.

Balogh J. – Balogh P. 1992. The Oribatid Mites Genera of the World. Budapest: Hungarian Natural History Museum. 1-263

Balogh J. – Mahunka S. 1980. Atkák XV. - Acari XV. Budapest: Akadémiai Kiadó. 1-177

Bährmann R. 2000. Gerinctelen állatok határozója. Győr: Mezőgazda Kiadó. 76-81

Bellinger P.F. – Christiansen K.A. – Janssens F. 1996-2007. Checklist of the Collembola of the World. http://www.collembola.org

Beyer L. – Cordsen E. – Blume H.P. – Schleuss U. – Vogt B. – Wu Q. 1995. Soil organic matter composition in urbic anthrosols in the city of Kiel, NW-Germany, as revealed by wet chemistry and CMAS ^{13}C-NMR spectroscopy of whole soil samples. *Soil Technology* 9: 121-132

Buzás I. – Bálint, Sz. – Füleky Gy. – Győri D. – Hargitai L. – Kardos J. – Lukács A. – Molnár E. – Murányi A. – Osztoics A. – Pártay G. – Rédly L. – Szebeni Sz. 1988. Talaj- és agrokémiai vizsgálati módszerkönyv, A talajok fizikai- kémiai és kémiai vizsgálati módszerei. Budapest: Mezőgazda Kiadó. 151-172, 174-175, 89-96

Craul P. J. 1999. Urban Soils: Applications and Practices. New York: John Wiley. 366 p.

Erhard C. – Szeptycki A. 2002. Distribution of Protura along an urban gradient in Vienna. *Pedobiologia* 48/5-6: 445-452

FAO (Food and Agriculture Organization of the United Nations) 2006. Guidelines for soil description. Roma. ISBN 92-5-105521-1

Hoblyák J. 1978. Állatökológiai gyakorlatok. Budapest: Tankönyvkiadó. 99-101, 109-120

Hollis J.M. 1992. Proposal for the classification, description and mapping of soils in urban areas. *English Nature*, Peterborough. 39 p.

Lee J.H. – Park H.H. – Kang B. – Jung Ch. E. – Choi S.S. 1999. Comparison of Oribatid Mite (Acari: Oribatida) Communities among City, Suburban, and Natural Forest Ecosystems: Namsan, Kwangerung and Mt. Jumong. KLTER Annual Events. 1-12

Lorenz K. – Kandeler E. 2005. Biochemical characterisation of urban soil profiles from Stuttgart, Germany. *Soil Biology and Biochemistry* 37: 1373-1385

Magura T. – Tóthmérész B. – Hornung E. 2006. Az urbanizáció hatása a talajfelszíni ízeltlábúakra. *Magyar Tudomány* 6: 705-708

Marosi S. – Somogyi S. 1990. Magyarország kistájainak katasztere. Budapest: MTA FKI. 213-218

Mátyás C. 1996. Erdészeti ökológia. Budapest: Mezőgazda Kiadó. 69-70

Mclntyre N.E. – Rango J. – Fagan W. F. – Faeth S. H. 2001. Ground arthropod community structure in a heterogeneous urban environment. *Landscape and Urban Planning* 52: 257-274

Móczár L. 1962. Állatok gyűjtése. Budapest: Gondolat Kiadó. 94-102

Parisi V. – Menta C. – Gardi C. – Jacomini C. 2003. Evaluation of soil quality and biodiversity in Italy: the biological quality of soil index (QBS) approach. Agricultural Impacts on Soil Erosion and Soil Biodiversity: Developing Indicators for Policy Analysis. Rome: Proceedings from an OECD Expert Meeting. 1-12

Schleuss U. – Wu Q. – Blume H.P. 1998. Variability of soils in urban and periurban areas in Northern Germany. *Catena* 33: 255-270

Simpson T. 1996. Urban soils. In: McCall G.J.H. – De Mulder E.F.J. – Marker B.R. (eds.) Urban Geoscience, Rotterdam: A. A. Balkema. 35-61

Stanton N.L. 1979. Patterns of species diversity in temperate and tropical litter mites. *Ecology* 60:295-304

Stefanovits P. – Filep Gy. – Füleky Gy. 1999. Talajtan. Budapest: Mezőgazda Kiadó. 191-196

Szemerey T. 2004. Erdőtalaj meszezésének hatása egy bükkös faállomány páncélosatka faunájára (Acari: Oribatida). PhD thesis. Nyugat-Magyarországi Egyetem Erdőmérnöki Kar, Sopron. 68-69

van Straalen N.M. 1998. Evaluation of bioindicator systems derived from soil arthropod communities. *Applied Soil Ecology* 9: 429-437

Wallwork J.A. 1983. Oribatids in forest ecosystems. *Annu. Rev. Entomol.* 28: 109–130

Weigmann G. – Kratz, W. 1986. Oribatid mites in urban zones of West Berlin. *Biology and Fertility of Soils* 3/1-2: 81-84

Weigmann G. 2006. Hornmilben (Oribatida). In: Dahl M. (Ed.) Tierwelt Deutschlands 76. Keltern–Weiler: Goecke and Evers. 1-520

White C.S. – McDonnell M.J. 1988. Nitrogen cycling processes and soil characteristics in an urban versus rural forest. *Biogeochemistry* 5: 243–262

Journal of Env. Geogr. Vol. I. No. 1-2. pp. 23-30

CLIMATE CHANGE AND CHANGING LANDSCAPE – A COMPARATIVE EVALUATION ON CHINESE AND HUNGARIAN SAMPLE AREAS

Rakonczai, J.[1] – Li, J.[2] – Kovács, F.[1] – Gong, A-D.[2]

[1]University of Szeged, Department of Physical Geography and Geoinformatics. 6722 Egyetem u., Szeged, Hungary
[2]Beijing Normal University, Institute of Ressource Technology 100875 No.19. Xinijiekouwai Street, Haidian District, Beijing, China

Abstract

The effects of globalisation are becoming obvious not only in the world economy but in natural processes as well. Increase of deterioration of natural conditions result in more and more decrease of land and water resources. Some experts even suggest that the changing climate of the next several decades can result in the transformation of the natural landscape.
Human activities, global and regional changes of climate and land use destroy the ecological environment, which also make the service function of the local ecosystem damaged constantly. We can improve ecological security of an area through regional land use pattern optimizing. The physical geographical consequences of aridification might be described through the decrease of ground water level, the change of the biomass quantity and quality. Their spatial and temporal variation may reflect the intensity and strength of degradation.
Remote sensing is one of the best tools to follow these processes, applying different databases. Spatial analysis of the gained information may help us to delineate the areas potentially endangered by even a minor climate change.

Key words: aridification, remote sensing, ground water, biomass monitoring, landscape change, land use optimization

INTRODUCTION

In 1972 at the Stockholm Conference the warming atmosphere was only a hypothesis. At the time the 4th report of the Club of Rome also regarded the future damage of the ozone layer as a theoretical problem. Nowadays, however, we talk about the greenhouse effect, or about the 'ozone-hole' as if they were well-known environmental issues already for a long time. Thus, it is not surprising that at first we thought that certain processes might not be influenced by these global processes. Nowadays, however, more and more observational data prove that the effects of global changes can be detected at different places of the Earth lying far away from each other, and they all exhibit very similar transformations. For example, the sample areas demonstrated in the present study, are located at 7000 km from each other, but the characteristics of their changes show many similarities.

In the international scientific community the effects of global warming can mostly be observed in desertification and aridification processes. Though natural and anthropogenic factors caused significant landscape changes in the previous centuries, the climate change makes these changes possibly more quick in the future (Csatári B. 2004, Rakonczai J. 2006, Láng I. et al. 2007, Metz B. et al. 2007). There are several uncertainties, and we do not know which changes will be irreversible. Connections within the landscape system are very complicated, that is, in the course of our research we can only use "indicators" which can demonstrate the process related to changes.

The real problem is, however, whether the affected regions are able to adapt to the changes. Experiments, carried out on the sample areas, support the above mentioned changes, but the environmental policy decisions of the countries can only follow up the events. The social adaptation to the changes demands to be not only a passive observer of (or, to be astonished by) the processes, but to adjust our activities and cultivation to these changes.

Effects of landscape changes and assessment possibilities

Considering the analysis of more than one hundred years of data and the experienced definite fall in precipitation in the latest 20 years – that can be figured out more or less trend-like – we heard many times that aridification has been evolving in Hungary. Comprehensive national evaluations carried out by different methods show a significant – at least 40-50 mm – annual fall in precipitation during a century on a national scale and the latest wetter years did not change the decreasing nature of the trend. The effects of increasing temperatures, decreasing precipitation, decreasing groundwater levels and the change of soil moisture content are the most dominating landscape factors. Lack is even more significant in certain parts of the Great Hungarian Plain, mainly in the Danube-Tisza Interfluve (*Fig. 1*). In this case GIS and multispectral remote sensing are the best methods to follow landscape dynamic processes, applying different databases (Mezősi G. – Szatmári J. 1998, Rakonczai J. – Kovács F. 2006a).

Farming-Pastoral Zone of Northern China is a vulnerable ecotone, which can be comparable to population hunger zone of African Sahel (*Fig. 2*). The climate of the study area is changeable, distribution of precipitation is uneven, the vegetation is destroyed seriously, proportion of the desertificated area is large, the ecological environment is fragile. High-intensity human activities as the excess reclamation, grazing and excavation, destroy the ecological environment, especially the natural vegetation which makes the service function of the local ecosystem constantly damaged. For the special geographical position and ecological sheltering function, the construction and protection of ecological environment in the study area is important for farming, animal husbandry and sustainable development of not only the study area but as well in the adjoined Beijing-Tianjing area (Wang J. et al. 1999, Verburg P. H. et al. 2000).

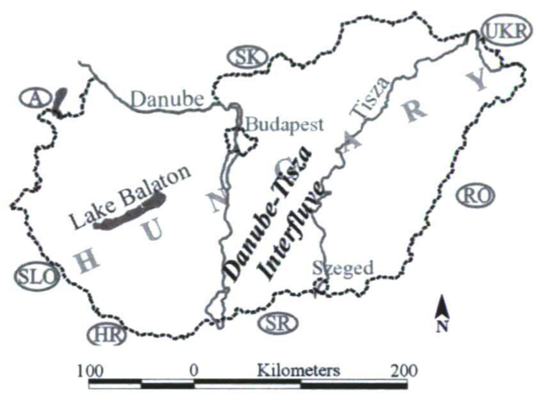

Fig. 1 The study area in Hungary

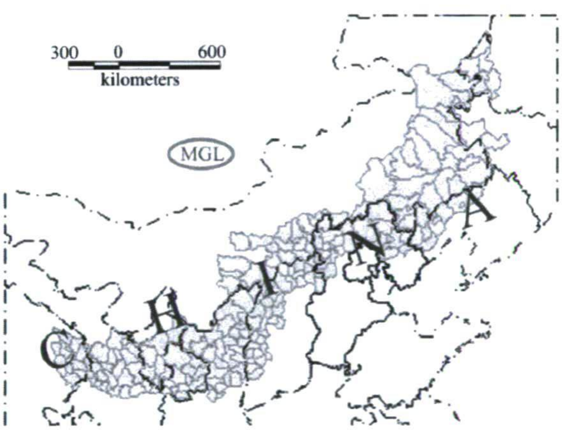

Fig. 2 The scope of the Farming-Pastoral Zone of Northern China

The essentials of land use pattern optimization are reasonable allocation of land resources and optimized landscape planning, which can harmonize the relationship of ecological, economic and social benefits (He C. et al. 2004). The LUOS model developed in the research overcomes all above limitation and considers synthetically the impact of natural and social factors on land use pattern optimization.

ENVIRONMENTAL CONSEQUENCES OF CHANGE IN WATER CYCLE – HUNGARIAN CASE STUDY

The change of natural water cycle is the most important factor in environmental changes which through several direct and indirect effects transform the characteristics of landscape components (*Fig. 3*).

Short term changes are evident: droughts and poor crop, floods, inland water. The most important long term effect is the decrease of ground water – though it is not obvious for the first sight. The decrease of ground water, however, influences processes through many interactions. On one hand, deeper groundwater level causes that vegetation can hardly reach and utilize it which results a decrease in biomass and in case of more significant transformation vegetation change can occur (on cultivated lands it forces the change of plants). On the other hand, the change of ground water modifies the vertical movement of water and salt in soils which results the genetic transformation of soils. In the consequences of this aridification processes may start or in case of arid soils it may generate a process that decreases salt. In both cases the change in the quality of the soil is accompanied with the transformation of the natural vegetation.

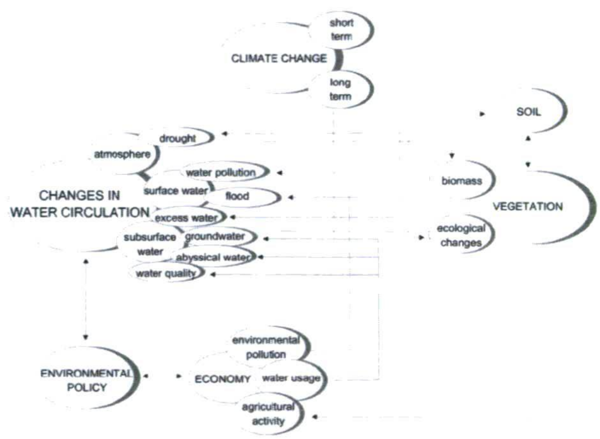

Fig. 3 The environmental consequences of the change of natural water cycle

Aridification as a geographical process with its direct consequences is hard to evaluate because there could be poor crop in a year with average rainfall as well, if the distribution of precipitation is unfavorable, respectively little rainfall can be replaced by irrigation. The complicated process is well-apprehensible when examining the year of 2000; in this year there were large areas covered by inland water at the end of winter and at the beginning of spring. There were great floods in the course of the year but later there was so serious lack of precipitation that the national precipitation average was around 400 mm which was unprecedented in the 20th century.

This is the reason why we looked for complex indicators in our research that do not investigate only one or another event (range of events) but are capable of signifying tendencies (as a matter of fact they are not infallible either).

Regional-size groundwater drop

Detailed research proved that the drop in rainfall was only one of the reasons of the change and it is a complex process in which social effects play important role besides natural elements. The most important factors that elicit aridification are as follows: lack of precipitation, increasing exploration of confined groundwater, frequent irrigation due to lack of precipitation, canals and other waterways and change in soil utilisation. On the Danube-Tisza Interfluve (where groundwater drop is the most relevant) there are about 500 measure stations on an area of 10.000 km^2 and more than half of them have data which can be used for long-term evaluation.

We analyzed the data of the wells by geoinformatic equipment and at the same time we checked their reliability by geostatistical methods. We can define the regional and temporal process of groundwater drop (*Fig. 4*) and besides we can produce exact figures with regard to the rate of water shortage.

The Danube-Tisza Interfluve, ascending between two great rivers as a ridge (the highest parts are higher by 40-80 m), and the subsurface water cycle of the area, namely the supply of groundwater, depends predominantly on precipitation. It has been found that, in the area mainly affected by the changes, decreasing groundwater is in close connection with the relief (orography) (Rakonczai J. 2006).

We could also realize that the supply of groundwater in particular parts of the area is in even closer connection with the meteorological relations; thus, a wetter period may help to re-establish its former state (*Fig. 5*). All this information, however, supports the idea that mainly the drier climate is responsible for the shortage. Several rainy years can reduce the water shortage of the area (*Table 1*), but there is an area of about 1500 km^2 where the rate of depression is so great that the process can hardly return to normal. The degree of aridification is well presented by the years of 1995 and 2003, when the decrease of ground water was 4.8 km^3, almost reaching (85%) the total water usage of Hungary.

The goal was to observe natural water resources through the dynamism of vegetation in a growing season from 1992 to 2005 with high temporal resolution AVHRR and MODIS images. The applied method of predicting net biomass production is the determination of the Normalized Vegetation Index (NDVI). Four major vegetation classes were examined (Kovács F. 2007).

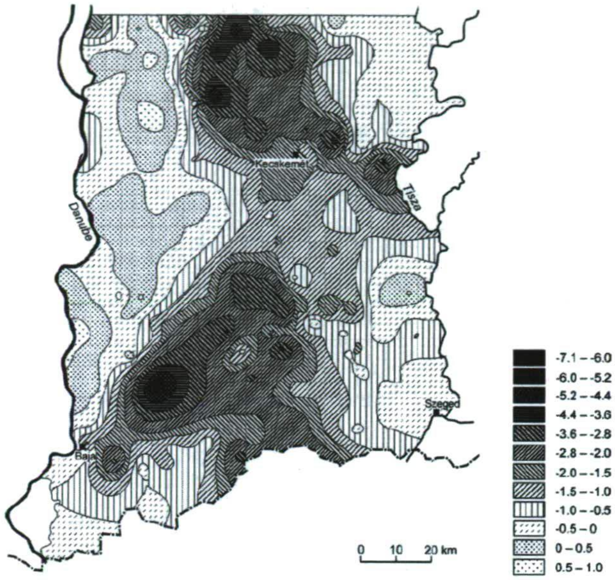

Fig. 4 The level of groundwater in March 2003 (in relation to the average of 1971-1975)

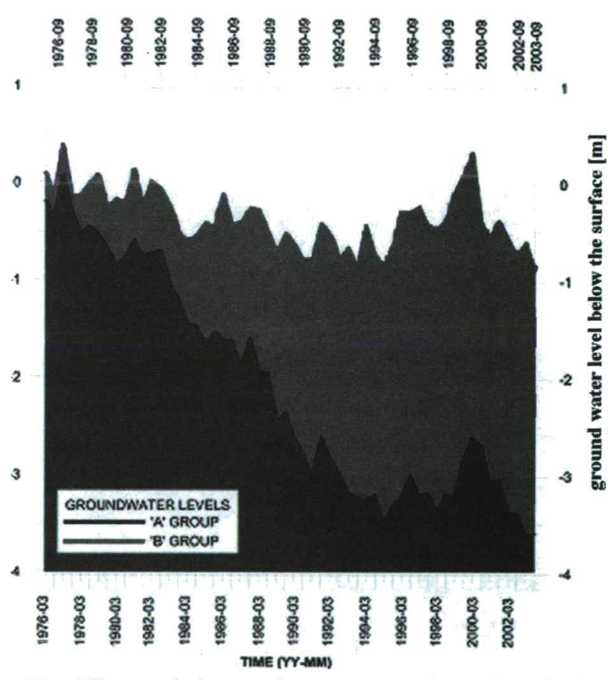

Fig. 5 Temporal change of average groundwater level in the two different types of landscape in the study area (in relation to the average of 1971-1975). Group A: wells that show significant decrease of soil water level; Group B: wells that have immediate hydraulic connections to the surface water supply (i.e. to the rivers)

Table 1 Approximate volumes of soil water deficit in relation to the early 1970's (1971-1975) in the Danube-Tisza Interfluve

Year	*Water deficit (km^3)*
1980	1,15
1985	2,32
1990	4,08
1995	4.80
2000	2,84
2003	4,81

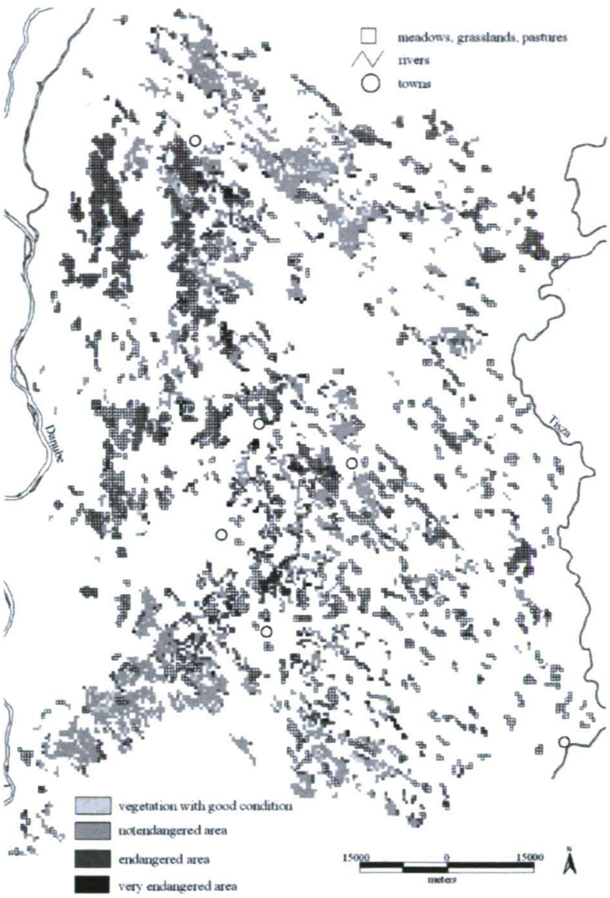

Fig. 6 NDVI-based regional distribution of the effects of aridification in the Danube-Tisza Interfluve

Regional multispectral biomass monitoring

Considering the distributions of precipitation, so-called average profiles were constructed for the individual classes on the basis of the average values of the wetter periods between 1996 and 1999, and 2001-2004. The spatial and temporal analysis of alterations from these average profiles may be used to determinate the dynamics of vegetation growth and to support the delineation of areas threatened by permanent biomass-loss.

A negative average NDVI data trend has been observed primarily in the months of April, July and September to 2003. The 10-15% changes in deep-rooted arboreal surfaces, within this short period, are very dangerous.

The amount of biomass produced is decreasing in one third of the vegetated area according to the spatial analysis of the 1992-2001 period. The reaction to the aridification process is unfavourable in one third of the mixed forests areas, in one fourth of the deciduous forests areas, one fifth of the coniferous areas and 42 % of grass-meadow-pasture areas.

The amount of produced biomass is decreasing by 16% in the vegetated areas as it was shown by the spatial analysis of the 2001-2004 period (*Fig. 6*). The response to the aridification process is unfavorable in one fifth of the mixed forest areas, in one seventh of the deciduous forest areas, in one third of the coniferous forest areas and in one seventh of grass-meadow-pasture areas.

A decreasing vegetation activity can be expected throughout the vegetation period with the exception of May, and according to the results derived by several approaches August-September can be regarded as a potentially imperiled month. The continously decreasing NDVI trend is very alarming in June and July, because these month are supposed to produce the greatest amount of biomass.

Landscape changes due to climate change

Between 1976 and 1978 we carried out detailed geographical research in the south-eastern part of Hungary, in the "puszta" (deserted area) near Szabadkígyós. We made an exact micro-morphological map on one of the characteristic alkaline benches of the area and together with botanists marked sample fields for mutual analysis (Rakonczai J. 1986). In the course of the measurements made in 2003 we could observe not only bench erosion but the change of vegetation and soil, too (Rakonczai J. – Kovács F. 2006b). The once eroded alkaline flats that were free of vegetation became covered by homogenous grass, bench erosion totally eliminated the former benches and grass and saline vegetation spots with static emerged, while bare alkaline surfaces disappeared. The permanent groundwater deficit caused a spectacular landscape change (*Fig. 7*).

SIMULATING LAND-USE PATTERN OPTIMIZATION IN NORTHERN CHINA

The emphases of land-use pattern optimizing simulation in the study area are gross demand controlling and spatial allocation (1km×1km), namely exact non-spatial simulation and spatial simulation (*Fig. 8*). In this case not only the optimized structure of land use in given conditions is well-known, but also its developing status, which results in the shortcomings of static research of normal linear planning (Jeffrey L. et al. 1997).

1986

2003

Fig. 7 Once sodic spots that became covered by grass during a quarter of a century in the "puszta" near Szabadkígyós.

According to the land resources characters of the study area and our research aim, six variables are set up which are cultivated land, forestland, grassland, water body, residential land and unused land, expressed with $x_1, x_2 \dots x_6$ respectively. Target function is set up on the basis of sustainable development (Eq. 1). The gross demand controlling scheme is the allocated result of all kinds of land-use types when function value reaches its maximum.

$$F(x) = 2180.068\, x_1 + 523.290\, x_2 + 733.885\, x_3 + 10567.339\, x_4 + 2507216.814\, x_5 + 68.283\, x_6 \qquad (1)$$

Spatially distributed combination of cell state is expressed by multidimensional integral matrix (*Fig. 9*).

In this study we used the 1989, 1994, 1999 NOAA/AVHRR remote sensing images, the meteorological data (precipitation, sunshine, temperature) of 194 observatories in 1961-2000 derived from Meteorological Administration, while statistical population data and other economic data of county areas regional in 1953, 1964, 1982, 1997, 2001 were provided by the National Bureau of Statistics of China.

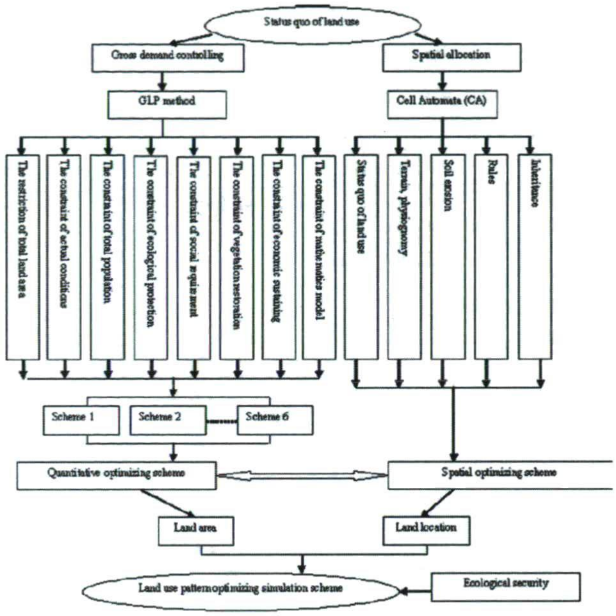

Fig. 8 LUOS model frame of land use pattern optimizing simulation under ecological security

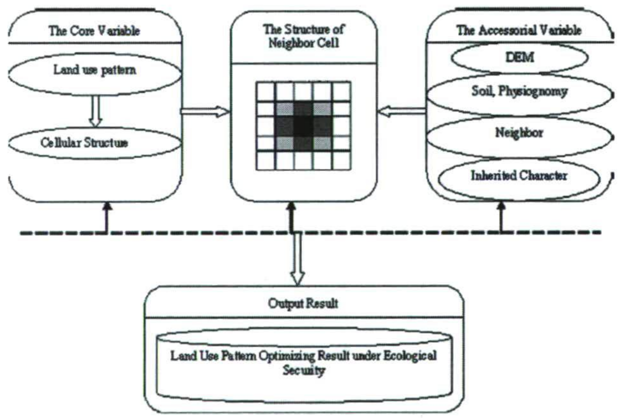

Fig. 9 The structure of the CA model

Results – Gross demand controlling

In line with actual conditions of the study area, we choose representative upper limit, lower limit and middle value of population and yield per hectare in GLP. Thus, we receive 9 types of optimizing schemes (*Table 2*). The population increasing speed of schemes 1, 2, 6 are 8.17‰, 8.43‰, 8.93‰, while those of schemes 3, 4, 5 are 8.17‰, 8.43‰, 8.93‰, respectively. Economic development speed is very fast and ecological environ-

Table 2 Comparison of all land use pattern optimizing simulation schemes

	Actuality	*Scheme 1*	*Scheme 2*	*Scheme 3*	*Scheme 4*	*Scheme 5*	*Scheme 6*	*Remark*
Population	71405938	78301350	81791975	78301350	81791975	82208977	82208977	
Yield kg/ha	1515	2100	2100	1890	1890	1890	2100	
Cultivated land (ha)	16850805	13054299	13627922	14500250	15146662	15223885	13701496	
Forestland (ha)	9264880	9264880	9268954	9268954	9264880	9264393	9264393	
Grassland (ha)	43039881	46817052	46235282	45367027	44720616	44643393	46165782	
Water body (ha)	79010	79010	79010	79010	79010	79010	79010	*
Residential land (ha)	72049	91384	95457	91384	95457	95944	95944	
Unused land (ha)	3342830	3342830	3342830	3342830	3342830	3342830	3342830	*

Note: * Supposed to be unchanged

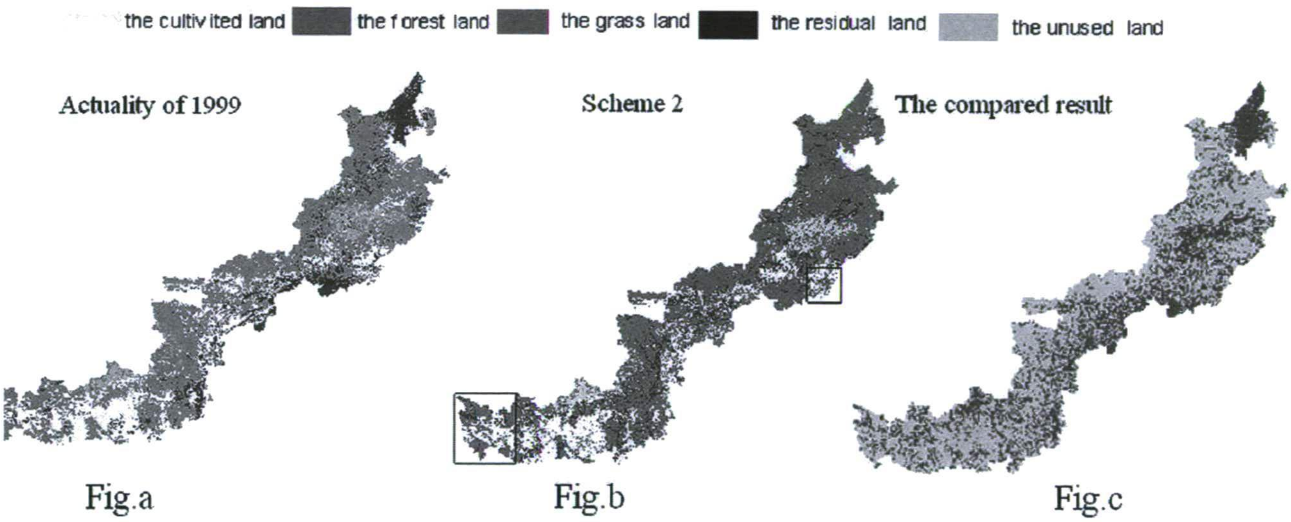

Fig. 10 The result of land-use pattern optimizing simulation

mental quality is relatively high in Scheme 1, which is difficult to be come true. Scheme 4 is similar to it except that the grain yield is less than the latter. Scheme 5 is alike to Scheme 2, the different of them is that the economic benefit of the former is worse than the latter. Controlling the population birthrate at 8.93‰, we can receive Scheme 3, the shortcoming of which is that the ecological benefit is not ideal. Economic, ecological and social benefit in Scheme 2 can be harmonized, which is an ideal optimizing scheme.

RESULTS – SPATIAL ALLOCATION

An ideal spatial distribution pattern map can be produced after the spatial calculation of CA module according to the gross demanding result of scheme 2 (*Fig. 10b*). The compared result map before and after land use pattern optimization is as *Fig. 10c*, which is the overlapped result of land use pattern optimizing result of scheme 2 and land-use actuality map. And the statistical result after comparison and analysis is as *Table 3*.

The amplificatory result map of *Fig. 10b*, as *Figs. 11a-b*, demonstrates that the cultivated land convert to forestland those gradient is steeper than 25°, which carry out the policy of cultivated land "grain for green" those gradient is steeper than 25°. This policy can reduce the phenomena of soil loss, land desertification and land quality descending. *Figs. 11c-d* are the demonstrations that residential land increases. The cells surrounding residential land cell can convert to other types of land in the order of grassland, cultivated land and forestland.

Table 3 Simulated land use conversions based on scheme 2

Type of conversion	*Area of converted land (ha)*	*Type of conversion*	*Area of converted land (ha)*
from cultivated land to forest	270870	from grassland to residential land	263520
from cultivated land to grassland	570389	from grassland to forest	111619
from cultivated land to residential land	2520	from forest to residential land	9975

DISCUSSION AND CONCLUSION

In the latest decade aridification could be observed in the Hungarian Great Plain not only because there has been a steady decrease in rainfall but it has multiplying effects. In the short run precipitation shortage can be measured in the annual change of the vegetation but permanent shortage could lead to regional groundwater deficit. This latest could elicit the genetic change of soils which could lead to the change of the natural vegetation even in a lifetime!

The negative effect rooting in destroyed ecological environment will spread to the whole North China, especially Beijing-Tianjin area, if current development ways continue. Thus, the land-use pattern optimizing simulation under ecological security condition is very important. The LUOS model can easily be applied to land-use pattern optimizing simulation of the study area.

From the point of view of remote sensing, the interesting qualitative parameters for the analysis of landscape change is quite limited, but can be more operative and expense-efficient in the future. For dynamic research, good time resolution earth observation remote sensing data are available, having more and more detailed spatial resolution (almost free data). Throughout a year some maximum value composite (MVC) images are

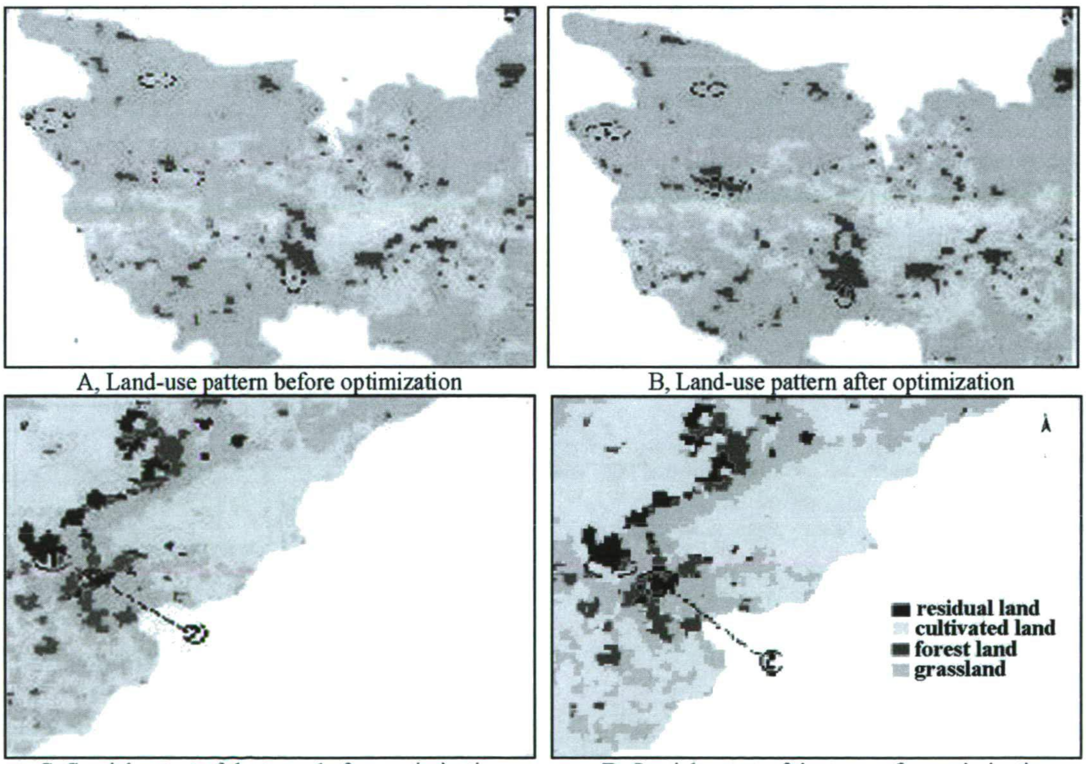

A, Land-use pattern before optimization B, Land-use pattern after optimization

C, Spatial extent of the town before optimization D, Spatial extent of the town after optimization

Fig. 11 Comparison of the simulated land-use distribution (cultivated land and residential land) before and after the optimization
Note: *Fig. a* and *b* correspond to the area 'a' of *Fig. 10b*. *Figs. c* and *d* correspond to the area 'b' of *Fig. 10b*

available offering good spatial data sampling which can be used well in the dynamic analysis even in areas of heterogeneous land use, on the regional scale. Our opinion is that this is the best possibility to observe the spatial and temporal evaluation of the effects of climate change on the landscape. We propose to develop a regional geographical monitoring, which could apply the methods introduced in this paper. The elements of the constructed system are the database–use and methods–evaluation, which could be supported with low expenses during operation. The new perspective for the future in long-term multi-spectral analysis is the development of connection between the data of different satellite images, making possible to use high temporal resolution images with high spatial resolution images (e.g. MODIS-LANDSAT).

The system is open. Therefore, it can be developed to be more objective with the assessment of other effectively endangered areas and with other landscape factors. Naturally, we can use the available spatial or statistical data, and this is one of the greatest possibilities of GIS in the complex geographical analysis. One example of application is the digital surface model, what we can use in the multidisciplinary examinations of longer and better time resolution data: i.e. meteorological indices or groundwater data. The more different data compared the more objective the results will be, but we must give greater importance to some dominant landscape factor (e.g. precipitation, wetness conditions, land use).

We need immediate arrangement and action to keep back waters and to make the water compensation stronger in the area and to validate the national decision. From geographical viewpoint the Danube-Tisza Interfluve and Northern China are sensitive areas, therefore the climatic effects and the unjudicious anthropogenic activity are very dangerous and increase the effect each one other. They also cause irreversible processes in the strongly protected and in quasi-native areas.

Acknowledgement

This study has been financially supported by the Hungarian Scientific Research Found (No. T048400) and O.A.S.I.S. program from SPOT.

References

Csatári B. (ed.) 2004. Homokhátság 2004, szembesítés, lehetőségek, teendők. Kecskemét: MTA RKK ATI. 35

He C. – Shi P. – Li J. 2004. Scenarios simulation land use in the northern China by system dynamic model. *ACTA Geographica Sinica* 59/4: 599-607.

Jeffrey L.A. – Darek J.N. 1997. Clarification on the use of linear programming and GIS for land-use modeling. *International Journal Geographical Information Science* 11/4: 397-402

Láng I. – Csete L. – Jolánkai M. (eds.) 2007. A globális klímaváltozás: hazai hatások és válaszok, a VAHAVA jelentés. Budapest: Szaktudás Kiadó Ház. 220

Metz B. et al. (eds.) 2007. Climate change 2007: Mitigation. Contribution of Working group III to the Fourth Assessment Report of the IPCC. Cambridge: University Press. 125

Mezősi G. – Szatmári J. 1998. Assessment of wind erosion risk on the agricultural area of the southern part of Hungary. *Journal of Hazardous Materials* 61: 139-153

Rakonczai J. 1986. A Szabadkígyósi puszta földtani viszonyai és geomorfológiája. *Környezet- és Természetvédelmi évkönyv 6.* Békéscsaba. 7-18

Rakonczai J. 2006. Klímaváltozás-aridifikáció-változó tájak. In: Kiss A. – Mezősi G. – Sümeghy Z. (eds.) Landscape, Environment and society. Studies in honour of professor Ilona Bárány-Kevei on the ocassion of her birthday. Szeged: SzTE. 593-601

Rakonczai J. – Kovács F. 2006a. Evaluating the process of aridification on the example of the Danube-Tisza Interfluve. In: Halasi-Kun G. J. (ed.) Sustainable development in Central Europe. Pollution and water resources. Columbia University Seminar Proceedings. Vol. 36. 2004-2006. Pécs: HAS CRS, TRI. 107-116

Rakonczai J. – Kovács F. 2006b. A padkás erózió folyamata és mérése az Alföldön. *Agrokémia és Talajtan* 55/2: 329-346

Verburg P. H. – Chen Y. – Veldkamp T.A. 2000. Spatial explorations of land-use change and grain production in China. *Agriculture, Ecosystems and Environment* 82: 333-354

Wang J. – Xu X. – Liu P. 1999. Landuse and carrying capacity in ecotone between agriculture and animal husbandry in northern China. *Resource Science* 21/5: 19-24

Journal of Env. Geogr. Vol. I. No. 1-2. pp. 31-39

FLOODPLAIN AGGRADATION CAUSED BY THE HIGH MAGNITUDE FLOOD OF 2006 IN THE LOWER TISZA REGION, HUNGARY

Sándor, A.[1] **– Kiss, T.**[1]

[1]Department of Physical Geography and Geoinformatics, University of Szeged, H-6722 Szeged, Egyetem u. 2-6, Hungary
andrea.sandor@gmail.com, kisstimi@earth.geo.u-szeged.hu

Abstract

The area of floodplains in the Carpathian Basin was dramatically reduced as a result of river regulation works in the 19th century. Therefore, the accumulation processes were limited to the narrower floodplains. The aims of the presented study are to determine the rate of accumulation caused by a single flood event on the active, narrow floodplain of the Lower Tisza and to evaluate the relations between the aggradation, flow velocity during the peak of the flood and the canopy. The uncultivated lands in the study area cause increased roughness which decreased the velocity of the flood, influencing the rate of aggradation. The highest flow velocity was measured on points where the flood entered to the floodplain and at the foot of the levee. These points were characterised by thick (over 50 mm) and coarse sandy sediment. In the inner parts of the floodplain flood conductivity zones were formed, where the vegetational roughness was small. In the inner parts of the floodplain the rate of aggradation was influenced by the geomorphology and the vegetation density of the area.

Key words: Lower Tisza, floodplain, accumulation, flow velocity, roughness

INTRODUCTION

The rate of floodplain aggradation is important from the point of view of increasing flood hazard and the dispersion of pollutants during flood events. Therefore, the rate of accumulation caused by single floods is studied along several temperate zone rivers (Gomez B. et al. 1997, Asselmann N. E. M. – Middelkoop H. 1998, Nagy B. 2002, Steiger J. – Gurnell A. M. 2002, Benedetti M. M. 2003, Oroszi V. et al. 2006). The accumulation is affected by several different factors which differ in time and space. The most widely cited and probably the most important factor is the geomorphology of the floodplain (Cazanacli D. – Smith N. D. 1998, Baborowski M. et al. 2007), the roughness of the inundated area (Rátky I. – Farkas P. 2003, Werner M. F. G. et al. 2005) and its land use (Knox J. C. 2006). Most studies analyse the pattern of the sediment deposited by a single flood event (Walling D. E. – He Q. 1998, Gábris Gy. et al. 2002) and its grain-size distribution (Hughes D. A. – Lewin J. 1982, Zhao Y. et al. 1999), or the connection between the flow velocity and the deposited sediment (Wyzga B. 1999).

The flood in 2006 was the highest recorded flood since 1842, when the gauge station network was established along the River Tisza (at the study area – Mindszent – the former record, 1000 cm in 2000 was replaced by 1062 cm on April 21 2006). In this area recent accumulation processes were studied after the 1998-1999, 2000 and 2001 floods (Kiss T. – Fejes A.

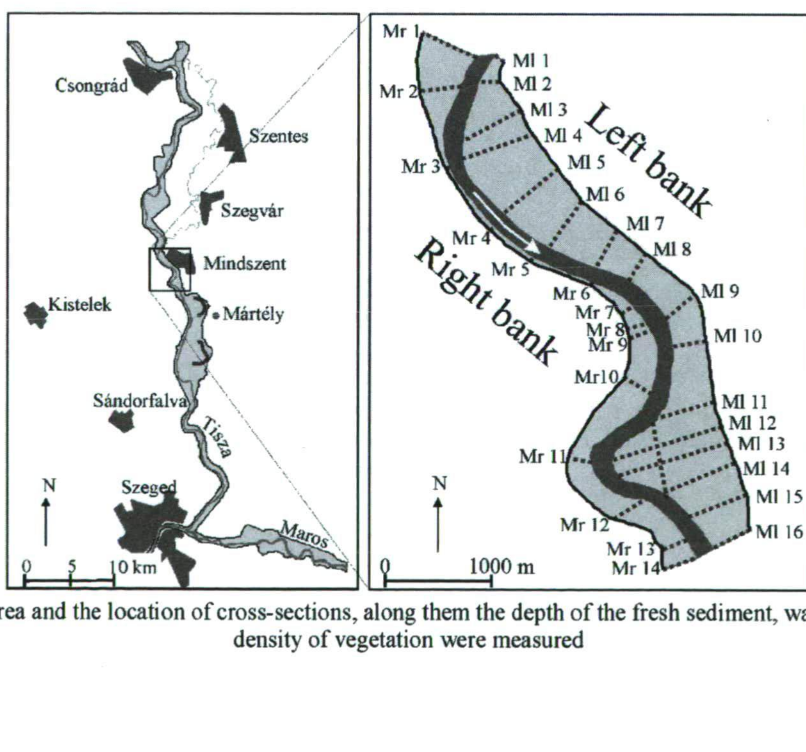

Fig. 1 The study area and the location of cross-sections, along them the depth of the fresh sediment, water velocity and the density of vegetation were measured

2000, Kiss T. et al. 2002). The aims of the present study are (1) to determine the accumulation rate caused by an extremely high flood and (2) to study the relationships between aggradation, flow velocity during peak flow and vegetation structure.

STUDY AREA AND THE 2006 FLOOD

The studied floodplain section is located in the Lower Tisza Region (*Fig. 1*), 6.5 km along the river (216.9-210.6 fkm), west of Mindszent. Here the River Tisza has three well-developed meanders; the lowermost is the sharpest. The artificial levees were built in 1890-1895, creating a narrow floodplain with quite irregular width, as the distance of the levee from the right bank varies between 35 and 560 m, while on the left side it is 110-1100 m respectively. The floodplain is flat, the difference in altitude slightly exceeds 2 m. The lowest features on the floodplain are swales and artificial sandpits and channels, and the higher ones are point bars and natural levees.

In the year 2006 two floods were recorded between April 10 and July 5 (*Fig. 2*). The first in April and May was 70-day-long, reaching a new record flood-level (1062 cm), and then a smaller and shorter flood-wave proceeded in June. The first was caused by the rapid snowmelt in the catchment and by the back-drainage of the Danube, while the second was due to high precipitation. Altogether the floodplain was covered by water for 102 days.

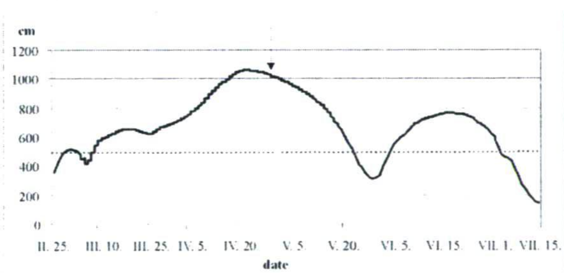

Fig. 2 Recorded water level at the Mindszent fluvio-meter in 2006 (data: www.vizadat.hu).
The arrow indicates flow velocity measure date

METHODS

Flow velocity measurements were carried out in order to determine the relation between flood flow and aggradation rate, and to reveal the role of vegetation in affecting flood flow. The number of flow velocity measurements were limited, as it had to be made within one day (April 30, 2006 at 1018 cm, just after the peak of the flood), because of the rapid falling. A calibrated Russian flow velocity meter (GR-21) was used from a motor boat, which was anchored. The measurements were made just on the left bank, along 12 cross-sections at 87 points. The exact location of each measurement-point was determined by Garmin GPS. Only at one point we measured the flow velocity at different depths to reveal the role of bushes in reducing flow. However, at each point we made only one measurement at the depth of 90 cm, partly because we wanted to make as many measurements as possible all over the floodplain, and partly because we could not hold it vertically in greater depth. The depth of the water column over the floodplain was 4.7 m in average (max. 5.2 m, min. 2.9 m).

At late summer the depth of the fresh sediment was measured along the same cross-sections as of the flow velocity measurements and along new cross-sections at both sides of the river (on ca. 500 points along 31 cross-sections). The leaf-layer of last autumn and the artificial surfaces created a reference level, therefore the depth of fresh sediment could be precisely measured. The grain-size distribution was determined by pipetten method and wet sieving.

Simultaneously with sediment measurements the arboreous vegetation of each point was described, namely species distribution and vegetation density. (Vegetation density was defined in different ways; their description can be seen below). In 3.0 x 3.0 m quadrates all the bushes and trees were counted and their periphery was measured at 1.0 m height. This mapping and the aerial photo, made in 2000, were used to create the canopy map of the area, using ArcView3.2. software. Based on the aerial photo the vegetation patches were identified, and based on the field measurements their average vegetation density was calculated.

Trees and bushes cover the largest proportion of the area (74.1%), and they play the most important role in increasing the roughness; therefore, these areas were classified from the point of view of flood conductivity. At first the quadrates were classified (*Table 1*) based on indices reflecting the number and size of trees. The *density index* was defined as the number of trees and bushes in the quadrate; the *periphery index* is the total sum of the periphery of the timber. In the final classification (*Table 2*) the above-mentioned two indices were summed (*canopy index*), but the density index was accentuated as according to our field observations it influences the flow velocity more.

In the quadrates belonging to the "sparse vegetation" class some old trees or in case of young planted forest no more than 10 trees grow, the underwood is sparse or missing. In the "dense vegetation" class at least 15 trees grow in a quadrate. These forests are undisturbed natural forests, planted poplar stands with sparse underwood. The "medium dense vegetation" category includes disturbed natural forests, poplar stands (at least 45 tree/bush per quadrate) and lands where *Amorpha* bushes appear. The "very dense vegetation" means all those areas (forests, former orchards and plough fields) which are overgrown by dense *Amorpha* bushes. Most of the study area (67%) belongs to the category of medium and very dense vegetation classes.

Table 1 Classes based on density and periphery indices

Density index	*Number of timber*
10	>45
9	41-45
8	36-40
7	31-35
6	26-30
5	21-25
4	16-20
3	11-15
2	6-10
1	1-5

Periphery index	*Sum of periphery (cm)*
5	>160
4	120-160
3	80-120
2	40-80
1	<40

Table 2 Vegetation classes based on the canopy index

Vegetation class	*Density index*	*Total periphery index*	*Canopy index*	*Number of quad-rates*
Sparse	1-2	1-2	2-4	13
Dense	3-4	1-3	4-6	6
Medium dense	3-7	1-4	6-9	22
Very dense	6-10	1-54	10-15	21

Vegetation classes were then converted into roughness categories (*Table 3*) in order to determinate the mean vegetational roughness of the floodplain, following the roughness categories of Manning (Chow V. T. 1959). However, these categories might vary by the level of the flood: during smaller floods the trunk of trees and bushes submerged increasing the roughness, but as the water-depth increases, free flood flow might occur over the dense bushes (Chow V. T. 1959, Németh E. 1959). Besides, the roughness changes within the same forest, as it is smaller on roads but greater on the boundaries.

Table 3 Roughness categories (after Chow V. T. 1959)

Category	*Type of vegetation/land use*	*Mean roughness (n)*
1	River channel	*0.03*
2	Short grass, dirty road	*0.03*
3	Cultivated plough-field	*0.035*
4	Cultivated orchard, uncultivated plough-field, clearings	*0.05*
5	Inundated shallow depressions (sand-pit, scour channel etc.)	*0.05*
6	Uncultivated orchard	*0.07*
7	Forest with sparse underwood	*0.12*
8	Dense forest dense *Amorpha* bushes	*0.2*

RESULTS

Vegetation of the study area in 2006

The largest proportion of the study area (74.1%) is covered by arbours: most of the forests (67.4%) have natural underwood and only 5.7% has a cleared ground without underwood. However, the land use of the floodplain differs at the two banks of the river: the right side is almost totally covered by forest (willow, poplar and the invasive *Amorpha fruticosa)*; but the left side is close to the town, therefore, cultivated areas (orchards 10% and plough fields 10.8%) also appear. However, after the great flood in 2006 many of the orchards and plough fields remained uncultivated (4.7% and 8.8%, respectively). On fields, which remained fallow land for few years (4.9%) invasive species (*Amorpha fruticosa, Echinocystis lobata*) create almost impenetrable stands.

The roughness (n) of the study area is between 0.03 and 0.2, the mean roughness is 0.13, which is considerably high, falling into the category of "forest with sparse underwood". Over half of the territory (60%) is covered by the two highest roughness categories (*Fig. 3*), and less than 10 % is under 0.035.

Flow velocity changes at the floodplain

Due to the limited number of velocity measurements, no velocity distribution map of the floodplain was made. The cross-sections will be presented, which are grouped based on the velocity distribution along them. Some has the highest flow velocity in the middle of the cross-section, while others have higher flow velocities at their ends.

The first group contains such cross-sections (MI-2, MI-5, M I-8 and M I-13), where high flow velocity was measured at the middle of the cross-section. Their length varies between 200 and 1080 m (*Table 4*). The most characteristic is the M l-13 cross-section (*Fig. 4*), which is located in the inner bend of the lowermost meander. At the foot of the levee, covered by grass (n=0.03), high flow velocity (0.6 m/s) was measured, but in the planted poplar stand with dense underwood (n=0.2) the flow velocity reduced remarkably (0.15 m/s). In the inner part of the cross-section higher velocities were measured over a road (0.32 m/s) and on the boundary between the bushes and the plough field (0.46 m/s). Over the immerged dense bushes no movement was detectable under the depth of 90 cm (at the level and below the top of the bushes), therefore, we made more measurements at this point to find out the vertical velocity distribution (*Fig. 5*). Flow velocity was above 0 m/s only over the immerged bushes: the highest velocity was measured at the surface (at 10 cm 0.13 m/s), then it decreased to 0 m/s at the depth of 70 cm. This information suggests that in very dense *Amorpha* stands (n=0.2) the roughness is so high that it prevents the waterflow and thus, it is only possible over the bushes. At the bank (on the point-bar) 0.21 m/s flow velocity was measured. The mean flow velocity of the cross-section was 0.18 m/s. The phenomenon, that relatively high flow velocity is typical in the middle of the cross-section, is in connection with flood conductivity routes. In these cases longitudinal patches with low vegetation roughness (road or forest clearings) or deeper swales between two former point-bars enabled faster flow (*Table 5*).

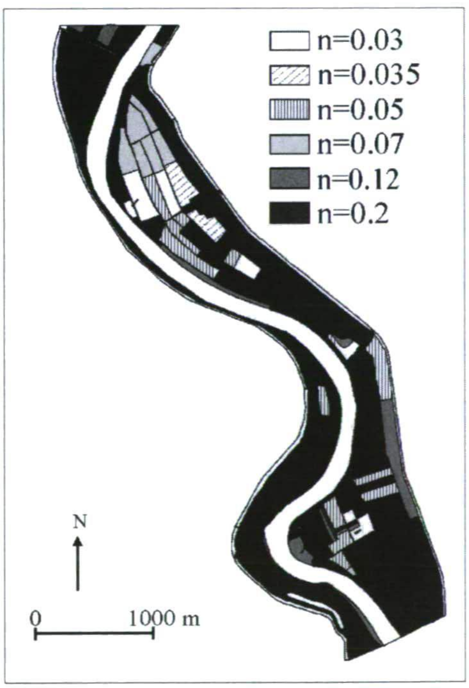

Fig. 3 Vegetation patches classified by their roughness (n)

Table 4 Data of cross-sections with high flow velocity in the middle

Cross-section	*Length (m)*	*Number of measurement points*	*Flow velocity (m/s)*			*Roughness (n)*
			min.	*mean*	*max.*	
M l-2	200	6	0	0.17	0.37	n=0.03-0.2
M l-5	650	11	0	0.15	0.62	n=0.03-0.2
M l-8	350	5	0	0.23	0.36	n=0.03-0.2
M l-13	1080	13	0	0.18	0.6	n=0.03-0.2

Table 5 Characteristics of the points situated in the middle of cross-sections and characterised by high flow velocity

Cross-section	*Description of the point*	*Distance from the river (m)*	*Flow velocity (m/s)*
M l-2	Road parallel to the river	55	0.37
M l-5	Low-lying surface, swale	305	0.37
M l-8	In clearings parallel to the river	103	0.36
M l-13	Road parallel to the river (2 points)	335 and 667	0.46 and 0.32

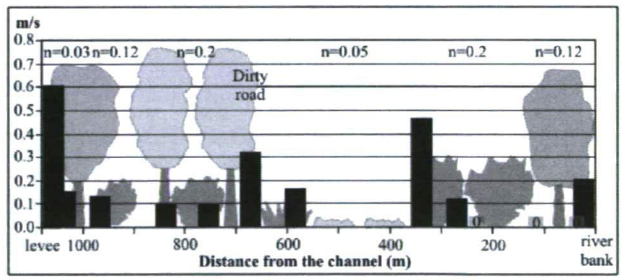

Fig. 4 Flow velocity distribution of the cross-section M l-13 (the vegetation type and the roughness are also indicated)

The second group of cross-sections is characterised by low flow velocity at their middle zones (M l-3, M l-6, M l-7, M l-9, M l-10 and M l-11). Their length varies between 330 and 630 cm (*Table 6*). The cross-section M l-6 is very typical for this group (*Fig 6*). Its length is 550 m, and the greatest flow velocity (0.56 m/s) was measured at the grass-covered levee (n=0.03). In the middle of the cross-section the roughness is higher (n=0.05-0.2), therefore, the flow velocity decreased to 0.12-0.2 m/s. Near the riverbank, in an old undisturbed gallery forest the flow velocity increased (0.53 m/s). The mean flow velocity of the cross-section is 0.22 m/s. In this cross-section group high flow velocity was typical at the river bank, partly because the morphological situation of the point (at inflexion and at convex bank, where the flood entered to the floodplain), and partly because the smaller roughness in forest with limited underwood or over the road running at the riverbank.

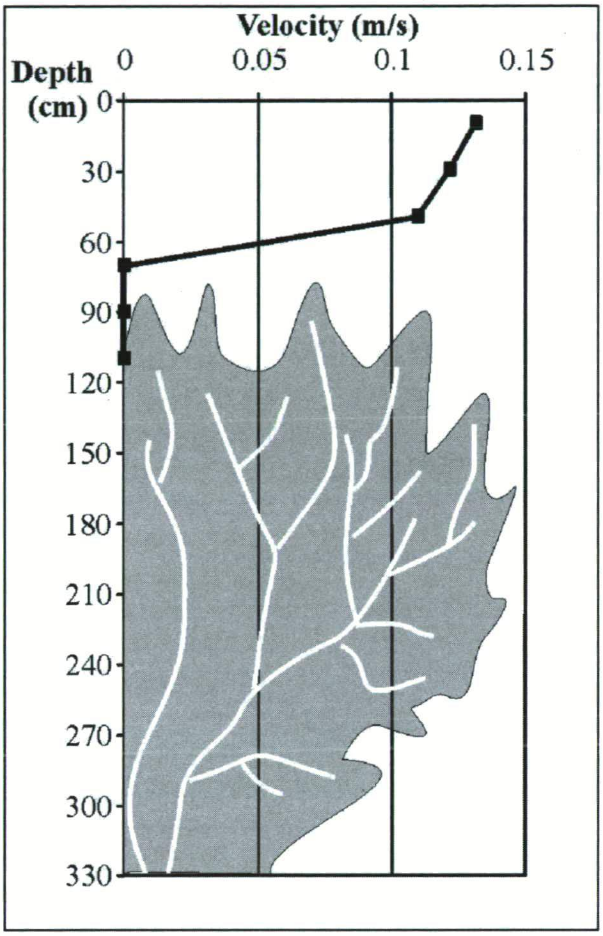

Fig. 5 Vertical velocity distribution over dense bush, at a point 225 m far from the channel

One longitudinal section (length: 680 m) was also made in the lowest and sharpest meander, between its inflexion points (*Fig. 7*). At the upper inflexion point, where the flood entered to the floodplain (forest clearance), the greatest flow velocity (0.55 m/s) of the section was measured. As the distance increased from the bank, the flow velocity decreased. Along the section the roughness was almost the same (n=0.03) as it was used as ploughland. However, on the edge of the ploughland and a forest (n=0.12-0.2) smaller flow velocity was measured. At the end of the section, at the riverbank flow velocity was again higher (0.37 m/s), though not as great as at the upper inflexion point. The mean flow velocity of this longitudinal section is 0.34 m/s, much higher than any of the cross-sections, showing the existence of a flood conductivity zone.

Table 6 Data of cross-sections with low flow velocity in the middle

Cross-section	*Lenght(m)*	*Number of sampling points*	*Flow velocity (m/s)*			*Roughness (n)*
			min.	*mean*	*max.*	
M I-3	630	9	0	0.22	0.28	n=0.03-0.2
M I-6	550	7	0.12	0.22	0.56	n=0.03-0.2
M I-7	415	6	0.1	0.17	0.3	n=0.03-0.2
M I-9	360	5	0	0.15	0.27	n=0.03-0.2
M I-10	320	6	0.07	0.27	0.4	n=0.03-0.2
M I-11	560	8	0.5	0.3	0.68	n=0.03-0.2

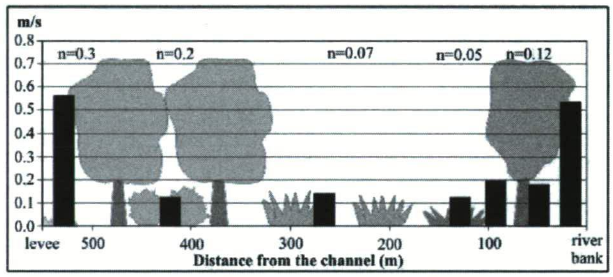

Fig. 6 Flow velocity distribution of the cross-section M I-6 (vegetation type and roughness are also indicated)

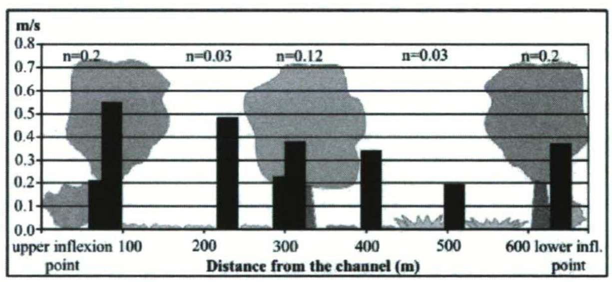

Fig. 7 Flow velocity distribution of the longitudinal section (vegetation type and roughness are also indicated)

Based on the results above, it can be stated that the greatest flow velocity on the floodplain is typical on patches running parallel to the river with low vegetational roughness, i.e. at the grassy levee, at roads and in poplar plantations with limited underwood. However, in areas invaded by *Amorpha* bushes the flow velocity drastically decreases, only over the bushes could the flood waterflow. Geomorphology of the riverbed determines where the flood can enter the floodplain, but in this case again the vegetation influences its efficiency. Morphology of the floodplain is also important as in the deeper swales, as well depending on vegetation conditions, greater flow velocity is typical.

Aggradation caused by the 2006 flood

The depth of deposited sediment was the greatest (50-500 mm) within 10-50 m from the channel. On the left side of the river, where the floodplain is narrow, the amount of aggraded sediment exponentially decreased with distance from the channel (*Fig. 8*), in accordance with earlier research (Walling D. E. – He Q. 1998). However, the left part of the floodplain is wider, therefore, the pattern of deposition was different, because other factors (geomorphology and vegetation) also influenced the aggradation. For example, we found patches with low aggradation rate. These areas were covered by very dense *Amorpha* bushes which acted as a barrier for the flowing water. Therefore, the water slowed down and even stopped among the bushes; thus, sedimentation took place on the boundary of the patch. The effect of floodplain geomorphology on aggradation was obvious where the floodplain was wide. In these cases thicker sediment was deposited in the deeper areas as in sand-pits, swallows and along a scour channel. At the points where the flood entered into the floodplain the aggradation was also greater.

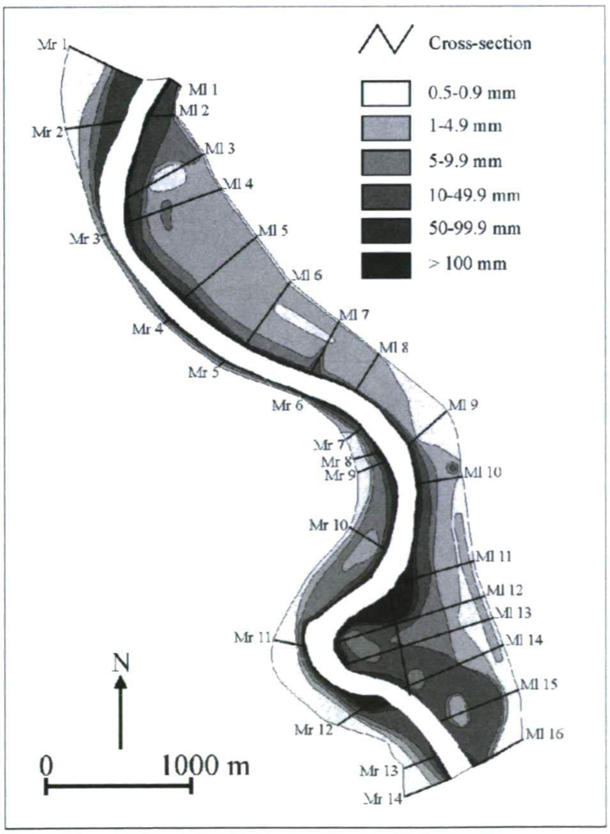

Fig. 8 Pattern of aggradation in the study area

The 31 cross-sections were grouped based on their length (*Table 7*). Group No. I contains those shorter than 150 m, while wider sections belong to the group No. II.

Table 7 Major characteristics of the studied cross-sections

Cross-section group			*Cross-section*	*Lenght (m)*	*Thickness of the fresh sediment (mm)*			*Mean flow velocity (m/s)*
					min.	*Mean*	*max.*	
No.I. Shorter than 150 m			M l-1	105	0.5	34.21	125	-
			Mr-3	45	0.5	1.45	6	-
			M r-4	60	0.5	22.43	135	-
			M r-5	60	0.5	10.76	70	-
			M r-6	35	0.5	49.91	130	-
			M r-7	143	0.5	30.81	230	-
No.II. Longer than 150 m	No.II/1. Exponential change of sedimentation		M l-4	710	0.5	9.3	260	-
			M l-11	555	0.5	45.93	150	0.3
			M r-1	560	0.5	7.14	48	-
			M r-2	400	0.5	2.98	15	-
			M r-9	220	0.5	13.59	500	-
			M r-10	300	0.5	5.99	186	-
			M r-11	230	0.5	19.25	500	-
			M r-12	353	0.5	65.15	250	-
	No.II/2. More peaks on sedimentation graph	II./2a	M l-3	625	0.5	8.11	200	0.22
			M l-5	675	0.5	5.45	120	0.15
			M l-8	310	0.5	8.77	144	0.15
			M l-9	370	0.5	13.82	280	0.15
			M l-10	330	0.5	18.04	170	0.27
			M l-12	1085	0.5	4.41	35	-
			M l-16	395	0.5	15.59	300	-
			M r-8	200	0.5	47.91	255	-
		II./2b	M l-6	550	0.5	6.16	140	0.22
			M l-14	750	0.5	7.75	80	0.09
			M r-13	250	0.5	4.71	90	-
			M r-14	347	0.5	34.44	280	-
		II./2c	M l-2	200	0.5	27.94	203	0.17
			M l-7	410	0.5	5.16	162	0.17
			M l-13	1080	0.5	12.61	150	0.18
			M l-15	585	0.5	8.33	20	-

The No. I. cross-section group includes the shortest ones (6). A typical example of this group is the Mr-4 cross-section which is only 58 m in length (*Fig. 9*). The greatest amount of sediment (135 mm) was deposited on the margin of the channel in a forest with very dense underwood. As far as 20 m from the channel the amount of accumulation was only 15 mm (decreased by 89%), and 50 m far it reduced to 3 mm. Here the aggradation from the channel towards the levee decreased exponentially (R^2=0.9182).

Group No. II. consists of cross-sections wider than 150 m (24). It was also divided based on the thickness changes of the sediment, namely whether it changed exponentially (No.II/1) or it had more peaks (No.II/2). Typical example for the first group is the Ml-11 cross-section starting from the upper inflexion point of the lowest meander (*Fig. 10*). Here the greatest amount (150 mm) of sediment was deposited within 180 m zone from the channel, in a poplar forest with dense *Amorpha* bushes. At 190 m from the channel the accumulation suddenly decreased (30 mm) at the border between a plough field and a dense scrub. Grain size distribution also changed, as on the banks the sediment consisted 95% sand, but at 190 m from the channel it was only 67%. Towards the levee thickness of the fresh deposit decreased and became finer.

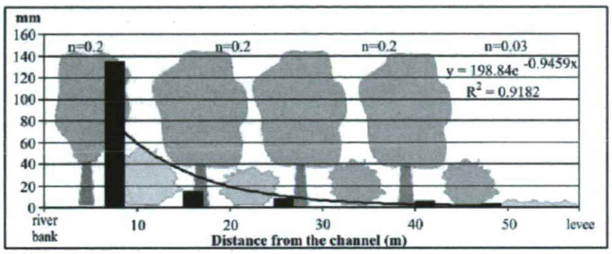

Fig. 9 Aggradation along the cross-section Mr-4

In some cross sections (No. II/2b) the maximum aggradation was measured at the channel and somewhere in the mid-zone of the cross-section. An example is the Mr-7 cross-section where 230 mm sediment was deposited on the bank (*Fig. 12*), but in 10 m it decreased to 180 mm, and in 25 m far it decreased further to 22 mm. From this point, increasing amount of sediment was measured (max. 60 mm) towards the levee.

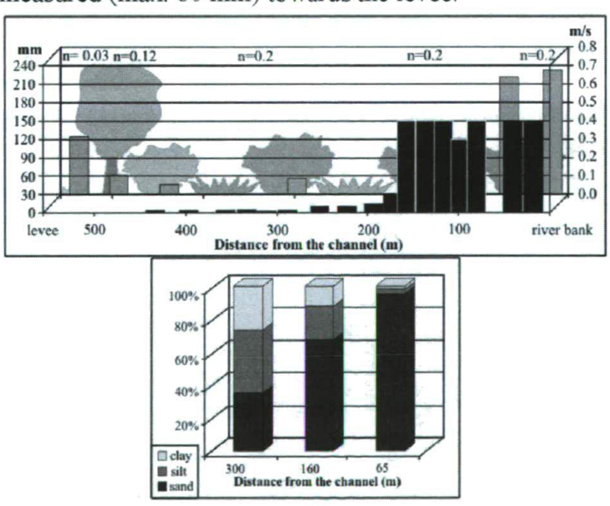

Fig. 10 Aggradation along the cross-section Ml-11 and the grain size distribution of sediment

In case of some cross-sections (i.e. No. II/2) more peaks appeared on the aggradation graphs. In some of them (No. II/2a) the greatest accumulation was measured at the bank and near the levee. One of them is the Ml-3 cross-section, where at the bank 200 mm thick sediment was deposited, but already at 40 m from the bank the sedimentation decreased to 38 mm, and at 150 m only to 6 mm, respectively (*Fig. 11*). In the middle part of the cross-section only very thin (less than 1 mm) sediment was deposited on a plough field. Near the levee (490 m far from the river) again thicker, 3-10 mm sediment accumulated in the deeper lying sand-pits.

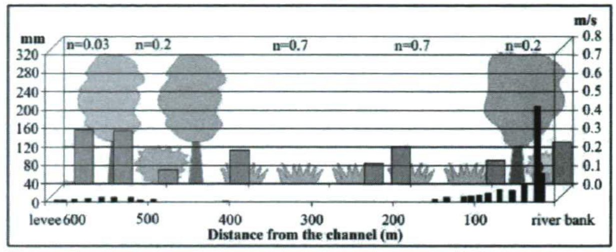

Fig. 11 Aggradation along the cross-section Ml-3

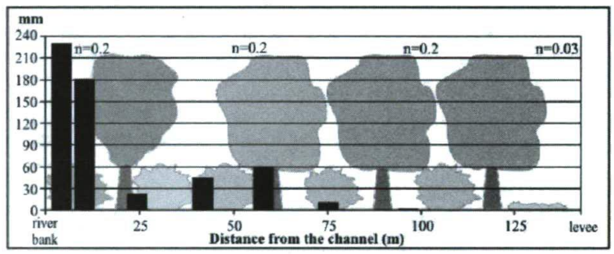

Fig. 12 Aggradation along the cross-section Mr-7

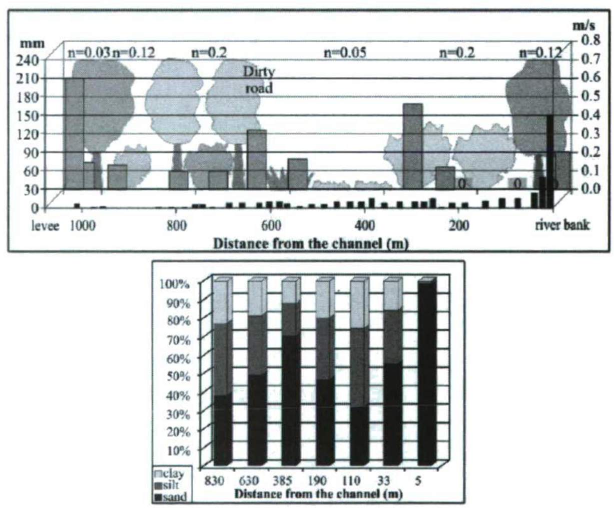

Fig. 13 Aggradation along the cross-section Ml -13 and the grain size distribution of sediment

Altogether four such cross-sections exist (No. II/2c) where three aggradation peaks were detected. For example, in the Ml-13 cross-section the accumulation rate decreased exponentially (from 150 mm to 8 mm) in 200 m from the bank (*Fig. 13*), and the sediment became finer. In the middle of the section (ca. 580-680 m from the channel) the amount of sediment increased (9-15 mm) and became coarser. The third sediment peak (3-7 mm) was measured in the sand-pit, near the levee, 950-1010 m far from the river. It suggests the existence of a flood conductivity zone; this fact, nevertheless, is also supported by the geomorphology (swale).

Based on the results listed above, it could be stated that the primary factor influencing the aggradation on the floodplain is the distance from the channel (*Fig. 14*). The greatest depth of sediment is deposited in form of point-bars and levees. From the banks the accumulation exponentially decreases towards the levees. The next factor is the pattern of the channel, as (1) where the water enters to the floodplain the aggradation is much higher compared to the neighbourhood, and (2) in case of the sharper bend the floodplain plays important role in flood conductivity, and therefore, in the flood conductivity zone more sediment was deposited.

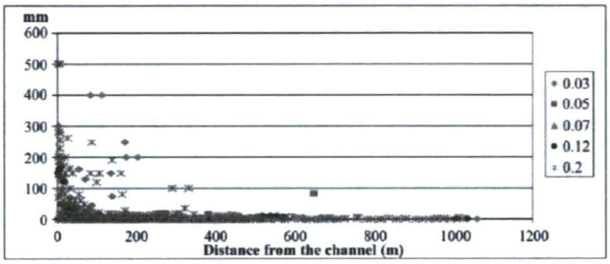

Fig. 14 Distance from the channel is plotted against the rate of accumulation in case of different roughness

Geomorphology belongs to the local factors influencing the rate of aggradation, as in deeper areas (e.g. swale, scour-channel and sand-pit) the accumulation is always greater. Far from the channel vegetation plays the most important role in the process of sedimentation. Here the very thick bushes prohibit the waterflow, thus the aggradation is smaller (less than 1 mm) than in areas at similar location (similar distance from the channel and similar geomorphological situation). Due to the above-mentioned local factors the exponential function can be applied only where the floodplain is narrow (max. 150 m).

The grain-size distribution of the sediment changes, as the sediment becomes finer departing from the channel. However, in flood conductivity zones coarser material was found in accordance with the flow velocity. The coarsest material is deposited in the area of natural levees and point bars.

CONCLUSION

The present land use of the area causes increased vegetational roughness (mean n=0.13), as 74% of the study area is covered by forest with dense underwood, uncultivated orchards and ploughlands. Increased roughness highly influences the waterflow: the denser the vegetation is the slower the waterflow on the floodplain becomes. The highest flow velocity is typical at those points where the flood enters the floodplain and at the foot of the levee. On the floodplain, where the roughness is small and therefore flow velocity is high, flood conductivity zones are formed running parallel with the river.

The rate of aggradation is primarily determined by the distance from the channel. The thickest (over 50 mm) and coarsest (95% of sand) sediment is deposited within 10-50 m from the channel, in the zone of point-bars and natural levees, independent of vegetation. The sediment became finer and the rate of aggradation decreased with the distance from the channel. In the flood conductivity zones, which run parallel with the channel and where the vegetation is sparse, thicker and coarser sediment was deposited.

In the narrow floodplain sections the rate of aggradation fits the exponential curve (R^2=0.8-0.9) as it was described in previous studies. However, where the floodplain is wider than 150 m, the aggradation is influenced by not only the distance from the channel, but also by the geomorphology of the area and the density of vegetation.

The pattern of fresh sediment follows the channel; however, in the southern sharp bend the flood makes a "short-cut", as it was ıeflected not only by higher flow velocity but also by greater aggradation. Patches characterised by small aggradation develops under very dense vegetation, where the flow velocity decreased to zero. It means that the very dense vegetation acts as a barrier against waterflow, therefore, sedimentary processes are more pronounced on their edges and much less sediment is deposited within.

Comparing these results with earlier measurements made in the same study site along the same cross-sections (Kiss T. – Fejes A. 2000, Kiss T. et al. 2002), we can state that the pattern of aggradation was very similar in each year. The rate of aggradation slightly differed, as in 2000 the mean accumulation on the floodplain was 20.5 mm (K.ss T. et al. 2002) and now it was 18.9 mm.

Acknowledgements

The work was financially supported by the OTKA 62200 research grant.

References

Asselmann N. E. M. – Middelkoop H. 1998. Temporal variability of contemporary floodplain sedimentation in the Rhine–Meuse delta, the Netherlands. *Earth Surface Processes and Landforms* 23: 595-609

Baborowski M. – Büttner O. – Morgenstern P. – Krüger F. – Lobe I. – Rupp H. – Tümpling W. V. 2007. Spatial and temporal variability of sediment deposition on artificial-lown traps in a floodplain of the River Elbe. *Elvironmental Pollution* 148: 770-778

Benedetti M. M. 2003. Controls on overbank deposition in the Upper Mississippi River. *Geomorphology* 56: 271-290

Cazanacli D. – Smith N. D. 1998. A study of morfology and texture of natural levee – Cumberland Marshes, Saskatchewan, Canada. *Geomorphology* 25: 43-55

Chow V. T. 1959. *Open Channel Hydraulics*. New York: McGraw-Hill. 89-127

Gábris Gy. – Telbisz T. – Nagy B. – Belardinelli E. 2002. A tiszai hullámtér feltöltődésének kérdése és az üledékképződés geomorfológiai alapjai. *Vízügyi Közlemények* 84: 305-322

Gomez B. – Phillips J. D. – Magilligan F. J. – James L. A. 1997. Floodplain sedimentation and sensitivity: Summer 1993 flood, upper Mississippi River valley. *Earth Surface Processes and Landforms* 22: 923-936

Hughes D.A. – Lewin J. 1982. A small-scale floodplain. *Sedimentology* 29: 891-895

Kiss T. – Fejes A. 2000. Flood caused sedimentation on the foreshore of the Tiver tisza. *Acta Geographica Szegediensis* 37: 51-55

Kiss T. – Sipos Gy. – Fiala K. 2002. Recens üledékfelhalmozódás sebességének vizsgálata az Alsó-Tiszán. *Vízügyi Közlemények* 84/3: 456-472

Knox J. C. 2006. Floodplain sedimentation in the Upper Mississippi Valley: Natural versus human accelerated. *Geomorphology* 79: 286-310

Nagy B. 2002. A felső-Tiszai árvizek kialakulásának tényezői, különös tekintettel az utóbbi évek katasztrófáira, illetve azok elhárításának lehetőségeire. Beregszász [Beregovo, Ukraine]: manuscript. 40-47

Németh E. 1959. *Hidrológia és hidrometria.* Budapest: Tankönyvkiadó. 161-210

Oroszi V. Gy. – Kiss T. – Botlik A. 2006. A 2005. évi tavaszi áradás üledékfelhalmozó hatása a Maros hullámterén. III. Magyar Földrajzi Konferencia Budapest 2006. szeptember 6-7. CD-ROM. 1-12

Rátky I. – Farkas P. 2003. A növényzet hatása a hullámtér vízszállító képességére. *Vízügyi Közlemények* 85/2: 246-265

Steiger J. – Gurnell A. M. 2002. Spatial hydrogeomorphological influences on sediment and nutrient deposition in riparian zones: observations from the Garonne River, France. *Geomorphology* 49: 1-23

Walling D. E. – He Q. 1998: The spatial variability of overbank sedimentation on river floodplains. *Geomorphology* 24/2-3: 209-223

Werner M. G. F. – Hunter, N. M. – Bares, P. D. 2005. Identifiability of distributed floodplain roughness values in flood extent estimation. *Journal of Hydrology* 314: 139-157

Wyzga B. 1999. Estimating mean flow velocity in channel and floodplain areas and its use for explaining the pattern of overbank deposition and floodplain retention. *Geomorphology* 28: 281-297

Zhao Y. – Marriott S. – Rogers J. – Iwugo K. 1999. A preliminary study of heavy metal distribution on the floodplain of the River Severn, U.K. by a single flood event. *Science of the Total Environment* 243-244: 219-231

Journal of Env. Geogr. Vol. I. No. 1-2. pp. 41-51

CHANGES OF CROSS-SECTIONAL MORPHOLOGY AND CHANNEL CAPACITY DURING AN EXTREME FLOOD EVENT, LOWER TISZA AND MAROS RIVERS, HUNGARY

Sipos, Gy.[1] – Fiala, K.[2] – Kiss, T.[1]

[1]Department of Physical Geography and Geoinformatics, University of Szeged, H-6722 Szeged, Egyetem u. 2-6, Hungary, gyuri@earth.geo.u-szeged.hu, kisstimi@earth.geo.u-szeged.hu
[2]Directorate for Environmental Protection and Water Management of the Lower Tisza District, H-6720 Szeged, Stefánia 4, Hungary, FialaK@atikovizig.hu

Abstract

When examining the characteristics of individual floods Hungarian researchers primarily investigate hydrological and hydraulic processes, whilst the relation between flood events and morphological changes of the river-bed are widely ignored. The present research quantifies the morphological changes of two cross-sections of the lowland reaches of the River Tisza and its tributary, the River Maros, during a high magnitude flood which occurred in spring 2000. During the flood several key morphological cross-section variables (mean depth, channel bed elevation, maximum depth, cross-sectional area and channel capacity) were monitored. Relationships between these data and daily river stage height series of the flood and specific stream power were determined. Results suggest that the identified morphological changes highly affect the channel capacity of the two cross-sections during the flood event. The channel capacity changes (9-10%) were almost identical for both study sites. However, different morphological processes characterised the two cross-sections. We found that morphological parameters depend not only on the actual stream power, but the available amount of sediment for transport, the rate of stage and stream power change.

Keywords: flood, riverbed morphology, specific stream power, water conducting capacity

INTRODUCTION

As a consequence of continuous stage height and discharge monitoring since the end of the 19th century the hydrology of the major Hungarian rivers is fairly well known. Numerous authors have studied the hydrological characteristics of the floods occurring on the Tisza and Maros Rivers (Bogdánfy Ö. 1906, Károlyi Z. 1960a, Bezdán M. 1998, 1999, Vágás I. 2000, 2001, Illés L. et al. 2003). Vágás I. (1984) observed on the River Tisza that the peak stage heights of floods with similar discharges tend to increase since the beginning of the measurements. In order to explain these changes climatic, hydrological, and land use changes in the catchment were investigated (Nováky B. 2000, Rakonczai J. 2000, Somogyi S. 2000, Bodolainé Jakus E. 2003, Gönczy S. et al. 2004). Other studies put a special emphasis on the role of floodplain aggradation (Nagy I. et al. 2001, Gábris Gy. et al. 2002, Kiss T. et al. 2002, Sándor A. – Kiss T. 2006). However, morphological processes (e.g. bank erosion, incision or aggradation) acting in the river channel during floods have rarely been analysed on Hungarian Rivers, even though these processes also influence flood stages (Starosolszky Ö. 1956, Károlyi Z. 1960ab, Sipos Gy. et al. 2007). At the same time more channel survey and discharge data are available (Szlávik L. – Szekeres J. 2003), which could further help the analysis of morphological development.
It is widely accepted that the increasing bed load transport and intensive dune and bar migration during floods have an effect on cross-sectional area (Bogdánfy Ö. 1906, Németh E. 1954, Károlyi Z. 1960b). Thus, morphological changes may contribute to (i) the characteristic loop-like curve of stage-discharge relationships (Németh E. 1954), and (ii) the differences of mean flow velocity during the rising and falling limbs of floods (Németh E. 1929, Vágás I. 1984).

The present study analyses the channel cross-section evolution during an exceptional, high magnitude flood in 2000 at two gauging stations located on the Tisza and Maros Rivers. The aim of the research is to monitor and to quantify morphological changes at each cross-section, and to compare the two rivers with different hydrological characters. The analysis also can help to understand channel changes (channel capacity) during floods, and provide a further explanation for increasing flood levels at the same discharge.

STUDY SITES

The study sites are located on the lowland, sand-bedded reaches of the rivers Tisza and Maros (*Fig. 1A*). The channel cross-sections are at the Algyő (Tisza River) (*Fig. 1B)* and Makó (Maros River), *(Fig. 1C*) gauge stations. These sites were chosen because they are located on similar, lowland sections of the studied rivers. The need for comparison is also supported by the fact that both rivers were severely regulated, but gave different answers for human intervention (flood hazard has increased on the Tisza, but not on the Maros).

One reason for this can be that the two rivers show very different discharge and sediment regime, as it is shown in *Table 1.* Flood duration is significantly longer on the River Tisza (1.5-3 months) than on the Maros, being much flashier (1-2 weeks) (Török I. 1977, Andó L. 2002). The sediment regime of the two rivers is also different. Based on the total sediment loads, the Tisza transports significantly more suspended sediment. However, the specific suspended sediment load is almost three times more on the Maros than on the Tisza indicating greater sediment concentrations. In terms of bed load transport the difference between the two study sites is even more important, as both the total and the specific bed load are significantly higher on the River Maros.

The Algyő gauge station is located at a bridge on a straight section of the River Tisza between two meanders 191.8 river kilometres (rkm) upstream of the estuary (*Fig. 1B*). The bankfull width at the cross-section is 115 m. Based on the full series of measurements (1929-2000), the mean depth is 12.8 m, maximum depth is 18 m, and the thalweg is usually located in the middle of the cross-section, which is typical of inflectional reaches.

The Makó gauge station is located 24.6 rkm from the Maros estuary at the upstream end of a fairly long, straightened reach of the river (*Fig. 1C*). Bankfull width is 112 m, mean depth is 4.8 m. Averaging all the avai-

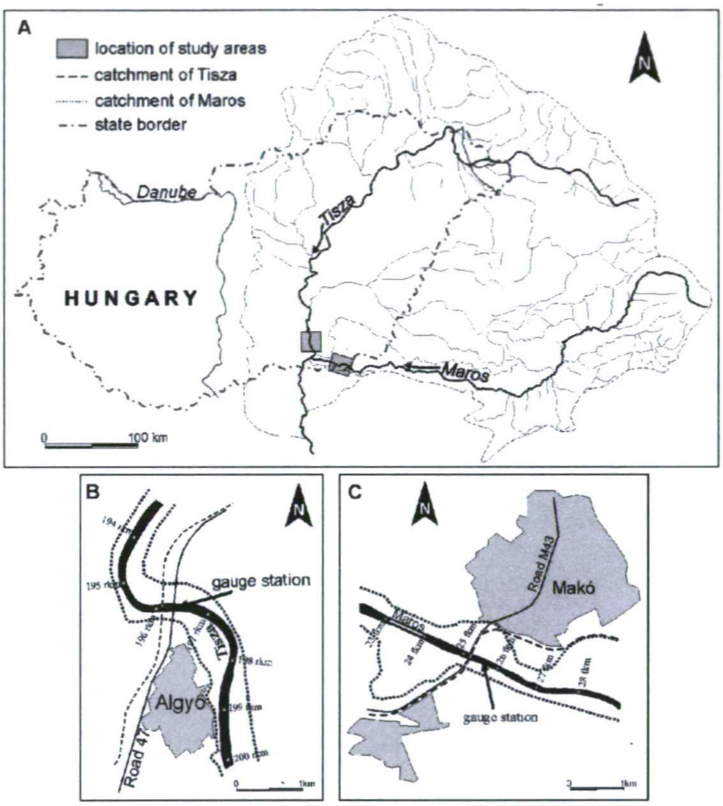

Fig. 1 The location of the studied reaches (A), and the locations of monitored gauge stations near Algyő (B) and Makó (C

Table 1 Characteristic stage, discharge and sediment load values at the Algyő (Tisza) and Makó (Maros) gauge stations. The specific sediment load (t/m^3) is sediment load (t/y) divided by mean discharge (m^3/s). (source of data: http://www.vizadat.hu and Bogárdi 1955, 1971)

		Tisza (Algyő)	Maros (Makó)
Stage height (cm)	maximum (1976-2000)	983	624
	mean (1976-2000)	284	36
	minimum (1976-2000)	-3	-104
	bankfull (2000)	610	310
Discharge (m^3/s)	maximum (1976-2000)	3 820	2 420
	mean (1976-2000)	930	161
	minimum (1976-2000)	63	34
	bankfull (2000)	2 020	850
Sediment load (t/y)	suspended load (1971)	18 700 000	8 300 000
	bed load (1971)	9 000	28 000
Specific sediment load** (t/m^3)	suspended load (1971)	$6,3x10^{11}$	$1,6x10^{12}$
	bed load (1971)	$3,1x10^{8}$	$5,5x10^{9}$

lable cross-sections (1988-2000), the "average" cross-section displays two troughs near the two banks and an elevation in the middle of the channel (*Fig. 7*). The cross-sections refer to frequent thalweg shifts and thalweg dissection.

METHODS

The stage and discharge data were provided by the ATIKÖVIZIG (Directorate for Environmental Protection and Water Management of the Lower Tisza District). Regular depth measurements, related to discharge monitoring, are similarly made by the ATIKÖVIZIG at the studied gauge stations since 1988. The endpoints of the cross-sections are stable survey-points and their geographic coordinates are determined. In case of the Tisza (Algyő site), water depth is determined from a bridge at 5 m intervals. On the Maros (Makó site) the measurements are made along a steel wire at 2 m intervals. Measurements are carried out on a monthly basis, except during flood events and extreme low water periods when discharge and water depths are monitored daily.

During the selected study period (February 01. 2000 – June 30. 2000) 35 water depth measurements were made on the River Tisza at the Algyő gauge station, and 28 on the River Maros at Makó. In order to follow morphological changes, reference water levels were set at both cross-sections. This reference level was bankfull water stage. It is relatively stable, clearly definable and has a geomorphic importance in terms of signing the stage at which the maximum stream power is exerted on unit area of the riverbed. As a consequence, the comparison of morphological changes became possible in between the two cross-sections as well.

The following morphological channel variables were calculated and monitored: mean depth [d_{mean}]; maximum depth [d_{max}], cross-sectional area [A], all measured from the bankfull level, and morphological roughness [r]. Roughness was defined as the morphological diversity of the riverbed. Its value was calculated as the summed difference between concomitant depth values [d] with the following roughness equation:

$$r = \sum_{i=0}^{n} \left| d_i - d_{i+1} \right|$$

This roughness index is not in relation with those derived from the grain size of riverbed sediments (e.g. Starosolszky Ö. 1970, Fehér F. et al. 1986). It evaluates the channel from the aspect of morphology, and thus it can be identified as form roughness (Nikora V. I. et al. 1998, Millar R. G. 1999).

Based on the dataset of stage variation different phases of the flood could be separated (rising stage, peak flow, falling stage). In order to analyse the different phases of the flood from the point of view of the changes in morphological parameters, the parameters were related to the daily rate of stage variation and specific stream power [ω]. Specific stream power enabled the comparison of the two rivers in terms of energy conditions during different flood phases. Specific stream power was determined according to Graf W. H. – Altinakar M. S. (1998):

$$\omega = Qsg\rho/w$$

where [Q] is discharge (m^3/s), [s] is water surface slope (m/m), [g] is gravitational acceleration (m/s^2), [ρ] is the summed density of liquid and solid phases (m^3/kg), and [w] is water surface width (m). Water surface slope was determined on the basis of stages measured at the studied gauge station and the closest station upstream (6 and 10 km). The floodplain component of width and discharge was disregarded, thus the specific stream power of the channel itself was determined.

CHARACTERISTICS OF STUDY PERIODS

In the spring 2000 a long-lasting flood period was detected in the eastern part of the Carpathian Basin, which could be divided into two main floods. An early spring smaller flood wave was followed by the main flood in May, when simultaneous, long-lasting floods developed on the River Tisza and its tributaries, including the River Maros (*Fig. 2*). The floods of both rivers were divided into differenat phases (*Fig. 3-4*) based on the direction of stage change.

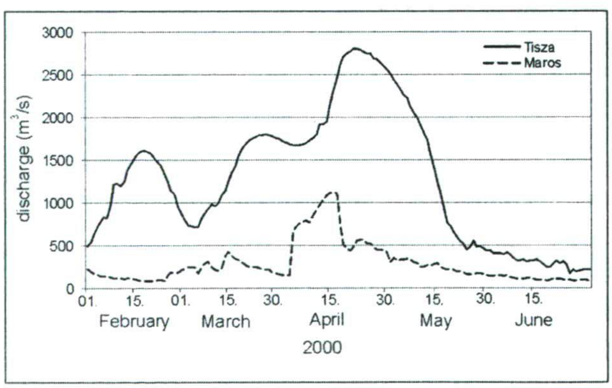

Fig. 2 Discharge curves of the 2000 flood at the Algyő (Tisza River) and the Makó (Maros River) cross-sections (source: Hydrological Year Book, calculated data)

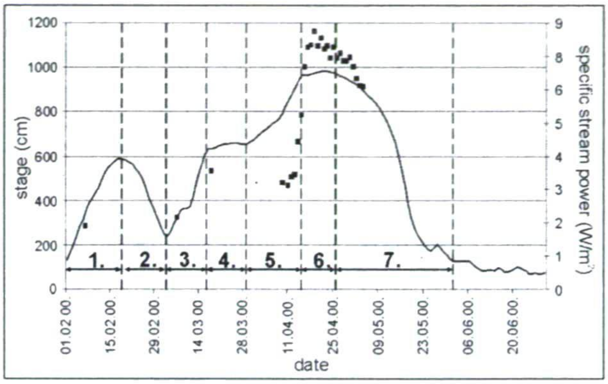

Fig. 3 Hydrograph (solid line) and specific stream power (squares) at the Algyő cross-section (Tisza). Black squares also indicate dates of channel cross-sectional measurements. Phases of floods are indicated as 1-7

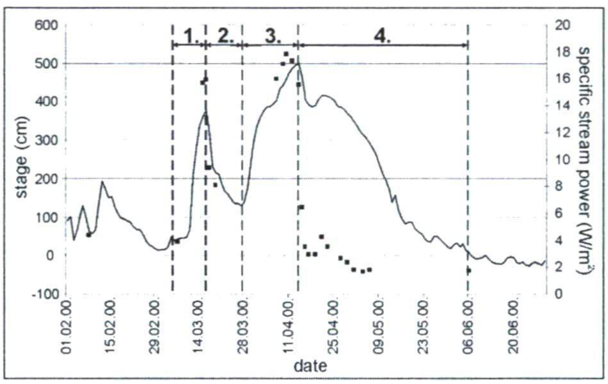

Fig. 4 Hydrograph (solid line) and calculated data of specific stream power (squares) at the Makó cross-section (Maros). Black squares also indicate dates of channel cross-sectional measurements. Phases of floods are indicated as 1-4

The first, early spring flood crest was reached after a very rapid stage rise on both rivers (Tisza: 32 cm/day in average, 39 cm/day maximum; Maros: 55 cm/day in average, 139 cm/day maximum). The flood on the River Tisza reached its crest earlier (phase 1; *Fig. 4*), on February 18 (Algyő: H=587 cm, Q=1610 m^3/s). On the River Maros the highest stage was measured one month later (phase 1-2; *Fig. 3*), on March 16 (Makó: H=378 cm, Q=345 m^3/s) (*Fig. 3-4*). Subsequently, a 17-day and an 11-day long intensive stage fall occurred on both rivers (Tisza: 23 cm/day; Maros: 24 cm/day). Along with the increase of discharge and water surface slope the value of specific stream power at the Makó gauge station (Maros) showed a sudden rise, reaching its maximum during the short peak stage (20 hours) period (ω=15,9 W/m^2). During the first, early spring flood no cross-sectional measurements were performed at Algyő (Tisza), thus no specific stream power could be calculated.

The second flood wave resulted in significantly higher stages on both rivers, at the Algyő gauge station (Tisza) even a new record was observed, since the beginning (1842) of the stage measurements. In the case of the Tisza the major flood, which started in March and terminated in May can be divided into five phases (phase 3-5; *Fig. 3*). First there was a quick stage rise between the 4 and 21 March (in average 24 cm/day, occasionally 66 cm/day), then an eight day long peak period came. Until April 21 another, less intensive rise occurred (in average 14 cm/day, occasionally 32 cm/day). Following the flood crest (H_{max}=983 cm, Q=2810 m^3/s) stage fell back to its pre-flood level in 42 days (in average 20 cm/day stage fall). Values of the specific stream power changed with stage variations. The maximum value (ω=7,3 W/m^2) was reached on April 19, two days before the peak flow arrived (*Fig. 3*). It can be explained by surface slope changes, as the greatest slope is measured before the flood crest.

In case of the Maros flood the rising limb of the second, major wave can be considered continuous (phase 3, *Fig. 4*). The rate of stage rise was similar to that of the Tisza (22 cm/day, occasionally 67 cm/day). The flood crest was reached in 18 days on April 14 (H=499 cm Q=1120 m^3/s), then it was followed by a relatively quick fall (15 cm/day), the continuity of which was disturbed by only a small late wave (*Fig. 4*). The maximum value of the specific stream power was reached four days before the peak flow period at the end of the rising limb (ω=17,8 W/m^2); later it decreased slowly (*Fig. 4*).

Hydrographs of the two rivers (*Fig. 3-4*) are similar in the number of flood crests; however, peak flow durations were much longer in the case of the Tisza than the Maros, and the Maros stage fall was more rapid (20 cm/day versus 15 cm/day). Energy conditions showed greater fluctuations at Makó (Maros) during the flood, and the maximum value of specific stream power was three times higher than in the case of Algyő (Tisza). Reasons were the significantly greater water surface slope and suspended load concentration apparent on the Maros. Another difference between the two rivers was that the maximum value of specific stream power occurred 2 days and 4 days before the peak flow of the main flood wave at Algyő and Makó, respectively (*Fig. 3-4*).

MORPHOLOGICAL CHANGES AT THE ALGYŐ CROSS-SECTION (TISZA)

First rising limb (Phase 1) and second rising limb (Phase 3)

During the first flood (February 1 – March 4) only one rising limb discharge measurement was performed, thus the exact description of morphological changes was not possible. However, the water-depth data obtained on February 7 could be compared to those measured during the rising limb of the main flood wave (*Fig. 6*), since the cross-section was recorded in both cases among similar stage and discharge conditions. Minor differences were experienced in terms of maximum depth (d_{max}=18.2 m, and d_{max}=18.5 m). The roughness index increased slightly (r=28.7 and r=29.2; see *Fig. 6*), as the specific stream power was also greater in phase 3 (February 8: 1.6 W/m^2, March 9: 2.0 W/m^2; see *Fig. 3*). However, in both cases the energy of the system increased suddenly due to intensive stage rise (36 cm/day and 30 cm/day).

Second rising limb (Phase 3) and first peak flow period (Phase 4)

During the first part of the main flood wave (March 4 to March 21) only two cross-sectional surveys were made (*Fig. 3*), one during the intensive rising limb and another during the 8-day long peak flow period.

Rising limb stage increase rate was 30 cm/day in average, with a maximum between March 12 and March 18 (44-66 cm/day). At that time relatively high maximum depth (d_{max}=18.5 m) and roughness index (r=29.2) characterised the channel (*Fig. 6*).

During the peak flow period (March 22-30) both maximum depth (d_{max}=18.0 m) and roughness (r=28.5) dropped, although specific stream power increased in the meantime from ω=2.0 W/m^2 to ω=3.5 W/m^2. Thus, we suggest that the morphological difference between the rising limb and peak flow channel can be independent from changes in the specific stream power.

Third rising limb (Phase 5)

Following a few days of stability water level started to rise again between March 31 and April 19 in the beginning at a rate of 12 cm/day but from April 10 at a rate of 30 cm/day. During this time mean and maximum depths

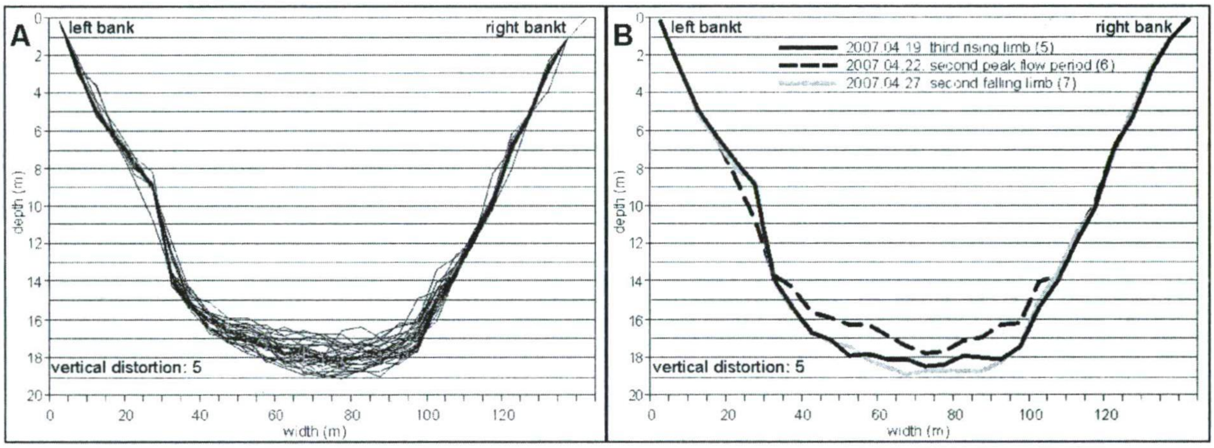

Fig. 5 (A) Monitored cross-channel sections (28) during the 2000 flood (February 8 – May 16) on the Tisza at Algyő. (B) Three characteristic cross-sections taken at different phases of the flood

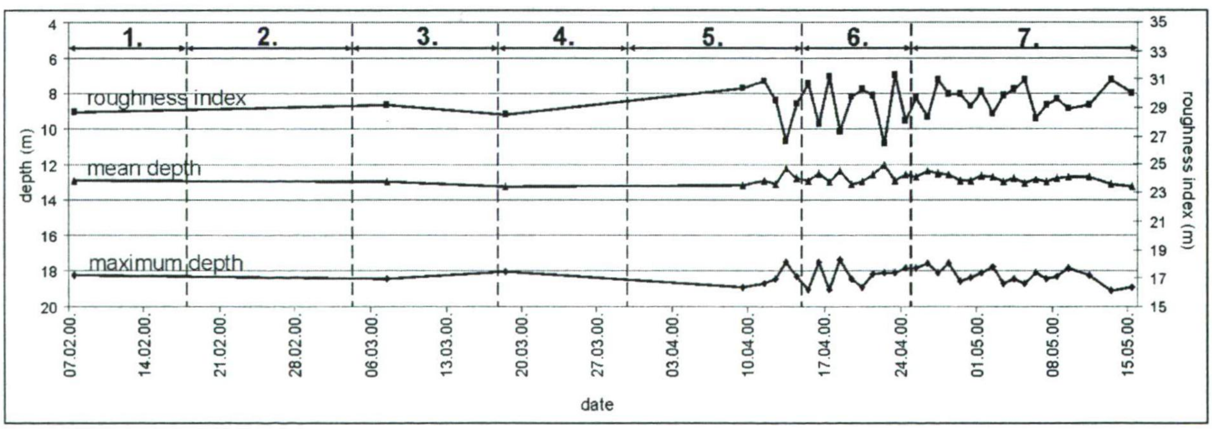

Fig. 6 Variation of morphological parameters during the 2000 flood at Algyő (Tisza). 1-7 indicates the different phases of the studied period

were increasing, however in a highly fluctuating manner (*Fig. 6*). The most intensive erosional activity can be related to this period, as the greatest mean and maximum depth values were measured on April 19 (d_{mean}= 13.1 m; d_{max}=19.1 m). Also, at this phase the roughness index of the riverbed reached its maximum (r=29.9 – 31.3) as dunes and dune sequences developed (Fig. 5B). The most probable reason for the river incision and intensive transportation is the greatest value of specific stream power during the flood (on April 19: ω=7.3 W/m²). Note, that the maximum of ω was experienced two days before the peak stage was reached, its reasons are also in relations with the watersurface slope increase before the flood crest.

Second peak flow period (Phase 6)

During the peak of the main flood wave (H_{max}=983 cm) the mean and maximum depth of the channel (d_{mean}=12.6 m and d_{max}=18.2 m) decreased by 10% (*Fig. 6*). In the background the decrease of stream power (from ω=6.9 W/m² to ω=6.5 W/m²) is the aggradation within the channel (*Fig. 3 and Fig. 5B*). As a result, the area of the cross-section decreased and reached its minimum value (A=1585.4 m²). In accordance to the aggradation the lowest roughness index was also experienced at this time (r=26.5 on April 22) meaning that r decreased by 10% compared to rising limb maximum values. These changes suggest that the intensity of sediment transport, initiated mainly during the rising limb, decreased significantly in the peak phase (*Fig. 5B*).

Second falling limb (Phase 7)

Subsequent to the 3-day long peak flow period starting on April 21, the water level started to fall at an increasing rate till May 14. In the first period of stage fall (7 cm/day) parallel with the decrease of specific stream power (*Fig. 3*) depth values dropped (d_{mean}=12.6 m; d_{max}= 17.6 m), i.e. the channel aggraded. Nevertheless, when stage fall became more intensive and reached values of 12 cm/day, erosion occurred again (*Fig. 5B and Fig. 6*). The process of channel incision was continuous (d_{mean}=13.0 m; d_{max} =19.1); therefore, cross-section area increased and reached its maximum (A=1742.6 m²). Roughness also increased (r=30.0), higher values were measured only during the most intensively rising days (*Fig. 6*). At the same time, the value of the specific stream power significantly decreased (from ω=6.4 W/m² to ω=5.5 W/m²).

MORPHOLOGICAL CHANGES AT THE MAKÓ CROSS-SECTION (MAROS)

First rising limb (Phase 1)

In the rising phase of the first flood wave (March 10-16) depth and roughness values increased significantly: mean depth by 11 cm (5%), maximum depth by 84 cm (21%) and the roughness index by nearly 50% (from r=13.4 to r=19.7) (*Fig. 8*). Overall, the channel deepened, while the riverbed was characterised by several half a meter-, meter-high forms, which can be interpreted as dunes developing due to the increase of stream power (*Fig. 7B*). In the meantime, by the disappearing of the right bank trough, no permanent thalweg could be identified in the channel. This phase occurred while a large quantity of bed sediment was entrained and started to move in the channel as a result of sudden specific stream power increase (from ω=3.9 W/m² to ω=15.9 W/m²) (*Fig 7B*).

First falling limb (Phase 2)

Right after the peak of the flood (March 16) as water surface slope and specific stream power decreased the

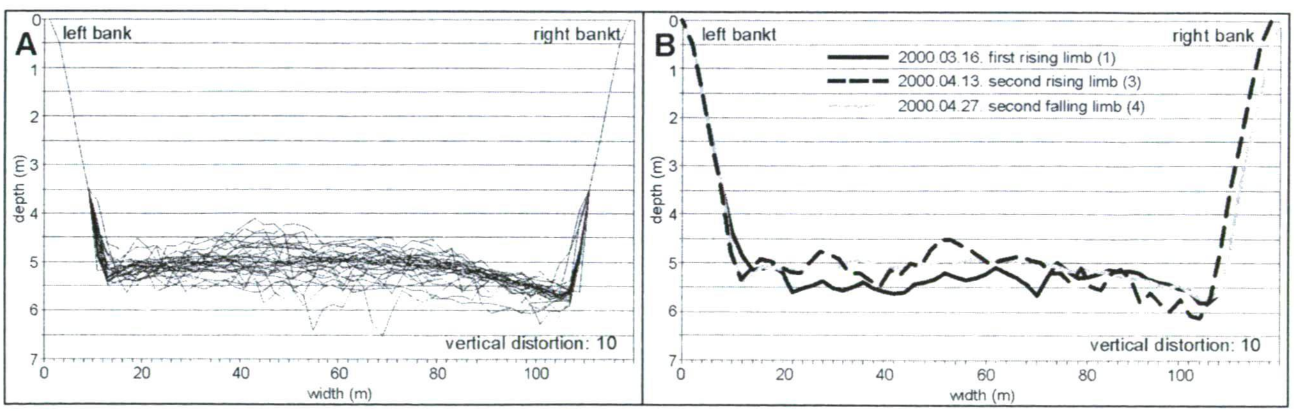

Fig. 7 (A) Monitored cross-channel sections (22) during the 2000 flood (February 8-June 6) on the Maros at Makó. (B) Three characteristic cross-sections taken at different phases of the flood

values of morphological indices dropped back suddenly. In 3 days mean depth and maximum depth decreased by 16 cm (6%) and 82 cm (21%), respectively. Thus, depth practically returned to pre-flood levels, unlike the roughness index, which did not reach its former value, and decreased from r=19.7 to only r=15.3 (*Fig. 8*). The slight decrease of roughness was due to the development of a positive form in the middle of the channel (*Fig 7A*). Based on one cross-section, it is not possible to describe the form; however, it seems as if the profile of a mid channel bar, formed from dunes overrunning each other due to the decrease of stream power (Nikora V. I. et al. 1997), can be observed.

Second rising limb (Phase 3)

During the first part of main flood wave stage rise (March 27-April 7) no measurements were made. The April 7 cross-section shows that the width of the mid channel accumulation increased up to 70-80 m. In the meantime, a small trough appeared at its axis; thus, roughness increased significantly again (r=17.8) (*Fig. 8)*. On the next day (April 8) the erosion of the trough was more expressed; in this way, actually, a third thalweg developed in the channel. In the following days, mean and maximum depth and roughness were fluctuating intensively (*Fig. 7A and Fig. 8*). Consequently, from a morphological aspect this phase of the flood can be considered as the phase of significant sediment relocation in the form of dunes and bars.

In terms of the second flood wave the greatest roughness (r=19.0) mean and maximum depth (d_{mean}=4.58 m, d_{max}=6.12 m) values were measured on April 13, one day before the peak stage (*Fig. 7B and Fig. 8*). Two important observations were made in connection with the above.

Firstly, the greatest morphological diversity and the maximum of specific stream power (April 10: r=16.1 m, d_{mean}=4.55 m, d_{max}=5.62 m) did not coincide (compare *Fig. 4 and Fig. 8*), and morphological indices were the highest when the value of ω already started to decrease (from 17.9 W/m^2 to 16.7 W/m^2). Secondly, even at this time depth values and roughness were significantly smaller than those experienced during the first flood wave, although at that time specific stream power was lower. Therefore, it is not at all obvious that the higher the specific stream power is the greater morphological diversity and cross-sectional area can be expected.

Another morphologically important pheno-menon was that during the rising limb of the second flood wave (April 7-April 14) the base level of the riverbed was 20-30, in some cases 50 cm higher than during the first flood. Thus, the second flood wave did not scour the channel bed, but probably it transported the previously relocated sediment in the form of dunes and bars (*Fig. 5B*). We suggest that, the gentler rise of stage during the second wave and the high volume of already entrained sediment from the upper sections explain the shallower riverbed.

Second falling limb (Phase 4)

The very short peak flow period (April 14) was followed by a rapid stage fall, during which mean depth decreased by 9 cm (4%) in 5 days; thus, in accordance with decreasing stream power the bed was filled up. Then due to a slight stage rise within the falling limb depth and roughness values increased a little (*Fig. 8*). However, on the basis of the April 23 and 29 cross-sections, later the bed became almost even, and roughness dropped to 71% of the maximum value. From a morphological aspect this is in connection with the disappearance of separate thalwegs (*Fig. 5B*). Nevertheless, depth values stayed almost

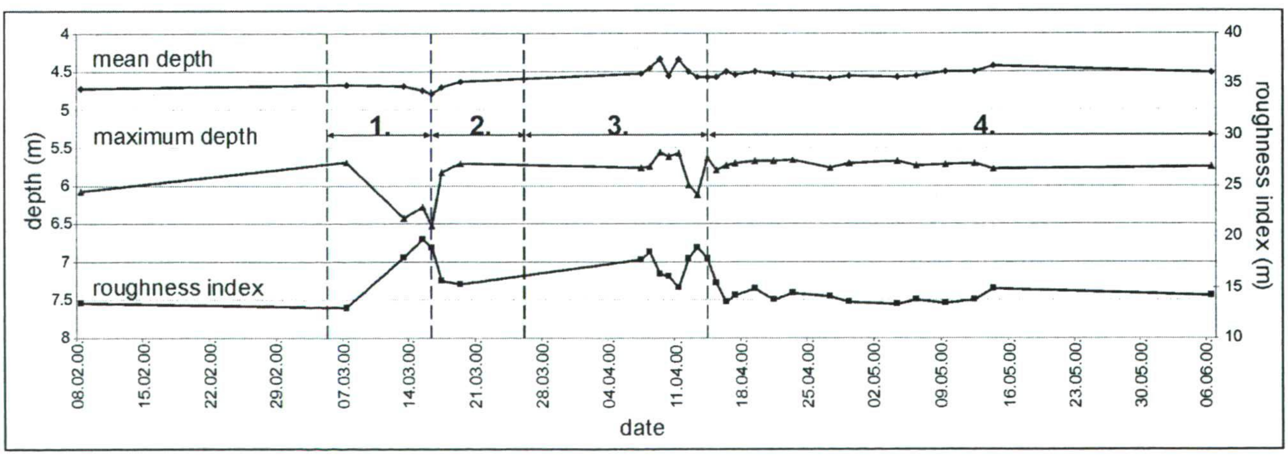

Fig. 8 Variation of morphological parameters during the 2000 flood at Makó (Maros). 1-4 indicate the different phases of the study period

the same during the late part of the falling limb. Finally, by the beginning of May a slight left bank accumulation appeared (side bar) and the thalweg returned to the right bank. If cross-sections taken right before and right after the 2000 spring flood are compared, then mean channel depth decreased by 18 cm (8%), maximum depth hardly changed (6 cm, 2%), and form roughness was very close to its original value (r=13.4 m before and r=14.1 m after).

CHANGES IN CHANNEL CAPACITY

The above-described morphological parameters also define the actual channel capacity of the two studied cross-sections. At the Algyő gauge station (Tisza) bankfull cross-sectional area significantly increased during stage rise (phase 1, 3 and 5; *Fig. 9*). In these phases the cross-section area and stream power increased simultaneously. However, the tendency of the area increase was characterised by significant variations. In some occasions a 6-7 % daily change was detected in cross-sectional area during the main flood wave. These processes indicate intensive morphological changes in the channel.

During the peak flow period depth values and the diversity of the riverbed significantly fell back, resulting the decrease of cross-sectional area and thus water conducting capacity (March 18 rising limb: A=1711 m^2; March 18, peak stage: A=1631 m^2). Minimum conductivity values occurred during maximum stage and discharge (April 21, peak stage: A=1585 m^2), when water surface slope and concomitant stream power decrease were apparent. It was also observed that the same values of stream power resulted in lower channel capacity during the peak flow period then during the rising limb (e.g. April 17, rising limb: ω=6.8 W/m^2, A=1715 m^2; while April 21 peak flow: ω=6.8 W/m^2, A=1585 m^2) (*Fig. 9*).

At the Algyő gauge station of the Tisza during stage fall depth and roughness increase were experienced. This resulted in a larger bankfull cross-sectional area and an increased water conducting capacity (April 25: A=1675 m^2, May 5: A=1714m^2). When stage fall became more intensive a significant fluctuation was observed; however, daily changes did not exceed 3%, representing continuous morpho-logical development, though less intensive than at the rising limb. In the meantime, along with the slow decline of discharge and slope the value of specific stream power also decreased (April 24: ω=6.5 W/m^2; May 4: ω=5.5 W/m^2) (*Fig. 3*). Consequently, a completely different relation was observed between stream power and conducting capacity than during the rising limb or at peak discharges (*Fig. 9*).

In terms of the Makó cross-section (Maros) the 2000 flood resulted in some similar situations. At the rising limb of the first flood wave similarly to the rising limb of the Tisza main flood wave bankfull cross-sectional area increased, however its degree was only 2%. The maximum channel capacity during the entire flood occurred at the peak of the first wave (March 16, short peak period: A=565 m^2) (*Fig. 10*). By the start of bar migration during the next rising limb, in spite of increased discharge and stream power bankfull area was decreasing. When the river reached its maximum specific stream power during the main flood wave (ω=17.8 W/m^2) cross-sectional area was 5% lower than in a similar period of the first wave (12.9 W/m^2). This contradicts the relationships experienced at Algyő, though there the work of the first flood wave could not be assessed precisely.

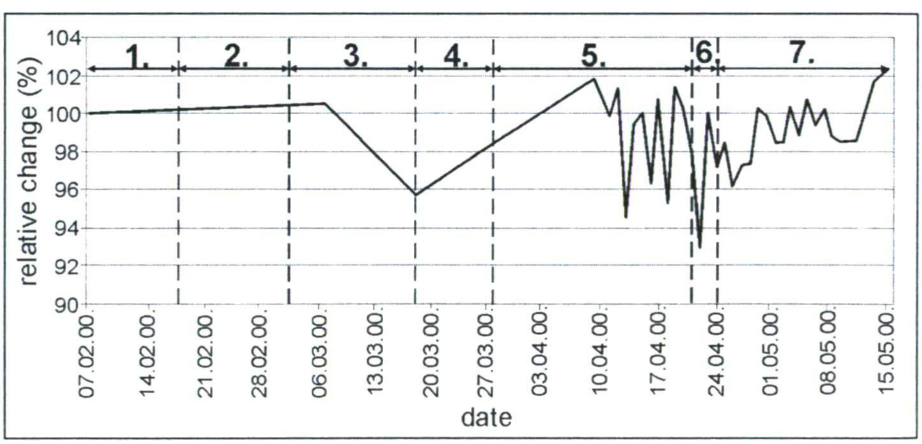

Fig. 9 Relative change of the bankfull cross-sectional area during the 2000 flood at Algyő, Tisza. Value of the first measurement was taken as 100%

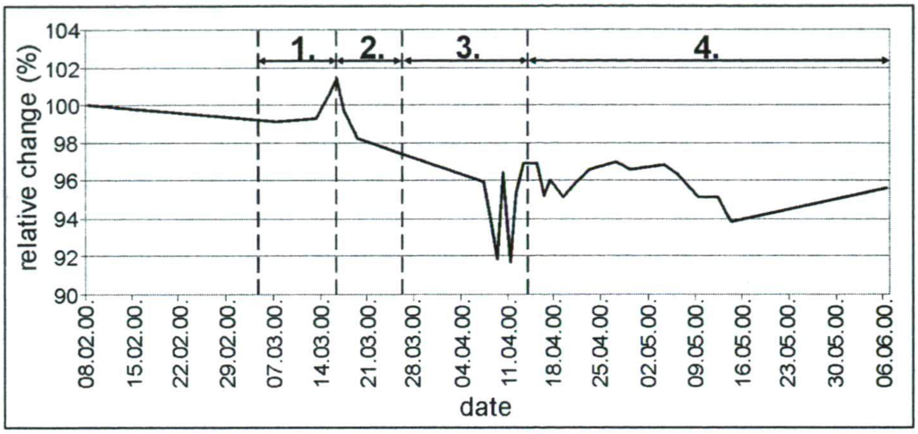

Fig. 10 Relative change of the bankfull cross-sectional area during the 2000 flood at Makó (River Maros). Value of the first measurement was taken as 100%

Following the short peak period of the Maros (20 hours) as stream power and roughness decreased no significant variation was detected in channel capacity (*Fig. 10*). At the end of the falling limb the bankfull area of the cross-section (A=533 m^2) was almost identical to the value observed during peak flow (April 19: A=530 m^2); however, by this time ω dropped to 1.68 W/m^2 which was only one tenth of the peak stage value. Consequently, morphological processes during the falling limb were different than at the Algyő cross-section. The possible reason for this is that the river due to the sudden loss of stream power was not able to transport further the bed load pulse initiated by higher energy periods. According to Sipos Gy. (2007), bedforms created by flood waves remain stable in the channel and for post-flood low waters it takes a relatively long time to restore the original bed state within the sand bedded River Maros.

The difference of the maximum and minimum cross-sectional area measured during the entire spring flood was 9.1% (ΔA=157 m^2) on the Tisza and 9.6% (ΔA=54 m^2) on the Maros. Thus, total variation was very similar (*Figs. 9-10*). In terms of maximum daily change, area difference was greater at Algyő (6.9%) than at Makó (5.1%). Nevertheless, variations during one day are not possible to determine at the present measurement frequency. Still, it seems well supported that relative variations in channel capacity were very similar at the two cross-section during the 2000 flood, despite of the fact that the maximum of specific stream power was 2.6 times greater in case of the Maros, and the standard deviation of these data was 6.2 at Makó, while it was only 1.8 at Algyő. The suggested reason why higher and more diverse stream power conditions did not cause greater morphological changes on the Maros is the remarkable volume of bed load (*Table 1*), which may buffer the energy variations of the river. However, the precise role of bed load in this respect is not possible to assess in detail because of the few number of sediment discharge measurements.

CONCLUSIONS

At both the Algyő cross-section of the Tisza and the Makó cross-section of the Maros significant morphological changes were observed during the 2000 flood. These changes greatly influence the channel capacity of the channel. Morphological development was compared to variations in specific stream power and the rate of stage rise or fall.

The way and degree of changes were different at the two sites. On the River Tisza at Algyő significant variations were experienced in depth and roughness during the rising limb, depending on the value of specific stream power and the intensity of stage rise. The overall process at this phase was the lowering of the bed level, thus the increase of channel capacity. During the days of the peak flow period, along with the sharp decrease of stream power the cross-sectional area decreased. This can be explained by the reduction of bed load transport and subsequent in channel aggradation. Nevertheless, at the falling limb of the flood in spite of the definite decrease of stream power depth increased again, and the area of the bankfull cross-section grew. In order to explain this controversy, further investigations are necessary.

On the River Maros, at Makó erosional activity was dominant only in the rising limb of the first flood wave. The greatest channel capacity was detected at this phase. Contrary to the processes at Algyő, during the main flood wave a continuous bed level rise was detected at Makó, even in case of periods with the highest energy levels. During the abrupt falling limb of the hydrograph the morphology of the channel settled, though depth values and bankfull cross-sectional area changed insignificantly.

Both the total and the daily variation of conducting capacity was similar at the two gauge stations, meaning a 9-10% difference between the maximum and the minimum cross-sectional area and a maximum 5-7% daily change. Similarity is striking considering that variation of specific stream power were much significant in the case of the Maros than on the Tisza (Makó $\omega_{max}/\omega_{min}$=10.6; Algyő $\omega_{max}/\omega_{min}$=4.6).

The paper proved the intensive cross-sectional changes during a flood, the processes outlined above show obviously a natural fluctuation. Therefore, based on only one flood it would not be sensible to generalise their role in the long term increase of flood levels. However, based on our present research, it is obvious that both in terms of the Tisza and the Maros the maximum of channel capacity usually will not coincide with maximum discharge and stage or maximum stream power. Therefore, morphological processes related to bed load transport can have a significant influence on peak stages and flood levels. Though earlier studies proved that the increasing bed load transport and intensive dune and bar migration during floods have an effect on cross-sectional area (Bogdánfy Ö. 1906, Németh E. 1954, Károlyi Z. 1960b), but could not calculate changes in detail. Our study proved that before the flood crest the specific stream power reaches its maximum, causing intensive scouring and bedload transport. However, at the period of flood crest the specific stream power is already decreased, therefore despite of former beliefs aggradation can truly overwhelm erosion at this phase, resulting significant channel capacity decrease. Earlier studies also over generalized the role of falling stages, supposing intensive aggradation; however, we proved that slow scouring can also occur in this period.

Acknowledgements

We wish to thank the ATIKÖVIZIG for providing the data of cross-sectional measurement. We are also grateful for the precious advice received on the May 2007 Budapest meeting of the Hungarian Hydrological Society. Our work was financially supported by the OTKA 62200 research grant.

References

Andó M. 2002. A Tisza vízrendszer hidrogeográfiája (The hydrogeography of the Tisza catchment). University of Szeged 143 p.

Bezdán M. 1998. Kölcsönhatások a Tisza-vízgyűjtő folyóin *Hidrológiai Közlöny* 78/4: 247-249

Bezdán M. 1999. A Tisza balparti mellékfolyóinak hatása az árhullámokra. *Hidrológiai Közlöny* 79/2: 89-99

Bodolainé Jakus E. 2003. Az 1998. évi őszi tiszai és más nagy árhullámok időjárási okairól. *Vízügyi Közlemények* 85, Special Issue I: 21-33

Bogárdi J. 1955. A hordalékmozgás elmélete. Budapest: Akadémiai Kiadó. 543 p.

Bogárdi J. 1971. Vízfolyások Hordalékszállítása. Budapest: Akadémiai Kiadó. 366 p.

Bogdánfy Ö. 1906. A természetes vízfolyások hidraulikája. Budapest: Franklin Társulat. 250 p.

Fehér F. – Horváth J. – Ondruss L. 1986. Területi vízrendezés. Budapest: Műszaki Könyvkiadó. 146 p.

Fiala K. – Kiss T. 2005. A középvízi meder változásai az 1890-es évektől az Alsó-Tiszán. *Hidrológiai Közlöny* 85/3: 60-68

Fiala K. – Sipos Gy. – Kiss T. – Lázár M. 2007. Morfológiai változások és a vízvezető képesség a Tisza algyői és a Maros makói szelvényében a 2000. évi árvíz kapcsán. *Hidrológiai Közlöny* 87/5: 37-46

Gábris Gy. – Telbisz T. – Nagy B. – Belardinelli E. 2002 A tiszai hullámtér feltöltődésének kérdése és az üledékképződés geomorfológiai alapjai. *Vízügyi Közlemények* 84/3: 305-322

Gönczy S. – Molnár J. – Szabó G. – Sándor A. 2004. Az erdőirtások hatása az árvízi vízhozamokra a Felső-Tisza kárpátaljai mellékfolyóin. *Földtani Kutatás* 41/3-4: 52-56

Graf W. H. – Altinakar M. S. 1998. Fluvial Hydraulics, flow and transport processes in channels of simple geometry. Chichester: Wiley. 506 p.

Illés L. – Konecsny K. – Kovács S. – Szlávik L. 2003. Az 1998. novemberi árhullám hidrológiája. *Vízügyi Közlemények* 85, Special Issue 1: 47-76

Károlyi Z. 1960a. A Tisza mederváltozásai – különös tekintettel az árvédelemre. Tanulmányok és kutatási eredmények 8. Budapest: VITUKI. 350 p.

Károlyi Z. 1960b. Zátonyvándorlás és gázlóalakulás - különös tekintettel a magyar Felső-Dunára. *Hidrológiai Közlöny* 40/5: 349-358

Kiss T. – Sipos Gy. – Fiala K. 2002. Recens üledékfelhalmozódás sebességének vizsgálata az Alsó-Tiszán. *Vízügyi Közlemények* 84/3: 456-472

Millar R. G. 1999. Grain and form resistance in gravel bed rivers. *Journal of Hydraulical Research* 37: 303-312

Nagy I. – Schweitzer F. – Alföldi L. 2001. A hullámtéri hordaléklerakódás (övzátony). *Vízügyi Közlemények* 83/4: 539-564

Németh E. 1929. Vízmérceállások és vízmennyiségek összefüggése. *Vízügyi Közlemények* 11/2: 41-66

Németh E. 1954. Hidrológia és hidrometria. Budapest: Tankönyvkiadó. 458 p.

Nikora V. I. – Sukhodolov A. N. – Rowinski P. M. 1997. Statistical sand wave dynamics in one-directional water flows. *Journal of Fluid Mechanics* 351: 17-39

Nováky B. 2000. Az éghajlatváltozás vízgazdálkodási hatásai. *Vízügyi Közlemények* 82/3-4: 418-448

Rakonczai J. 2000. A környezet hidrogeográfiai összefüggései az Alföldön. In: Pálfai I. (ed.) A víz szerepe és jelentősége az Alföldön. Békéscsaba: Nagyalföld Alapítvány. 16-27

Sipos Gy. 2007. A meder dinamikájának vizsgálata a Maros magyarországi szakaszán. PhD thesis. University of Szeged. 131 p.

Sándor A. – Kiss T. 2006. A hullámtéri üledék-felhalmozódás mértékének vizsgálata a Közép- és az Alsó-Tiszán. *Hidrológiai Közlöny* 86/2: 58-62

Sipos Gy. – Kiss T. – Fiala K. 2007. Morphological alterations due to channelization along the Lower Tisza and Maros Rivers. *Geographica Fisica e Dinamica Quaternaria* 30: 239-247.

Somogyi S. (ed.) 2000. A XIX. századi folyószabályozások és ármentesítések földrajzi és ökológiai hatásai Magyarországon. Budapest: MTA FKI. 310 p.

Starosolszky Ö. 1956. Az emberi beavatkozások hatása a vízfolyások morfológiai viszonyaira. *Vízügyi Közlemények* 38/2: 248-252

Starosolszky Ö. 1970. Vízépítési hidraulika. Budapest: Műszaki Kiadó. 355 p.

Szlávik L. – Szekeres J. 2003. Az árvízi vízhozammérések kiértékelésének eredményei és tapasztalatai (1998-2001). *Vízügyi Közlemények* 85, Special Issue 4: 45-59

Török I. (ed.) 1977. A Maros folyó 0–51,33 fkm közötti szakaszának szabályozási terve. Szeged: Alsótiszavidéki Vízügyi Igazgatóság. 119 p.

Vágás I. 1984. Az árvízi hurokgörbe. *Hidrológiai Közlöny* 64/6: 333-341

Vágás I. 2000. A Tisza és árvizei. *Hidrológiai Tájékoztató* 40/1: 45-50

Vágás I. 2001. Az ezredforduló árhullámai a Tiszán. *Magyar Tudomány* 48/8: 958-866